

STEROL SENSING BY TWO LUMINAL LOOPS IN SCAP

APPROVED BY COMMITTEE

Michael S. Brown, M.D. (Mentor) _____

Joseph L. Goldstein, M.D. (Mentor) _____

Philip J. Thomas, Ph.D. (Chair) _____

Joachim Seemann, Ph.D. _____

Michael Roth, Ph.D. _____

DEDICATION

This is dedicated to my wife, Lifen (Susie), and son, David (Muyi).

STEROL SENSING BY TWO LUMINAL LOOPS IN SCAP

by

YINXIN ZHANG

DISSERTATION

Presented to the Faculty of the Graduate School of Biomedical Sciences

The University of Texas Southwestern Medical Center at Dallas

In Partial Fulfillment of the Requirements

For the Degree of

DOCTOR OF PHILOSOPHY

The University of Texas Southwestern Medical Center at Dallas

Dallas, Texas

May, 2014

Copyright

by

Yinxin Zhang, 2014

All Rights Reserved

STEROL SENSING BY TWO LUMINAL LOOPS IN SCAP

Publication No: _____

Yinxin Zhang, Ph.D.

The University of Texas Southwestern Medical Center at Dallas, 2014

Supervising Professors: Michael S. Brown, M.D. and Joseph L. Goldstein, M.D.

SREBP cleavage-activating protein (Scap) is an endoplasmic reticulum (ER) membrane protein that controls cholesterol homeostasis by transporting SREBPs from the ER to the Golgi complex. Transport is initiated when COPII proteins bind to Scap and cause the Scap/SREBP complex to enter COPII coated vesicles for transport to the Golgi. In the Golgi complex, two proteases cleave SREBP, thereby releasing its transcriptionally active domain so that it can move to the nucleus and activate transcription of genes involved in cholesterol synthesis and uptake. Scap is not only an escort protein, but also a cholesterol sensor. When cholesterol is abundant in ER membranes, the sterol binds to Scap and triggers a conformational change in the protein that prevents COPII proteins from binding to Scap. The Scap/SREBP complex cannot move to the Golgi and proteolytic cleavage is terminated. This cholesterol feedback inhibition is essential to control cholesterol metabolism in animals.

Scap can be divided into two functional regions. The C-terminal cytosolic WD domain interacts with the regulatory domain of SREBPs. The N-terminal membrane attachment domain

includes eight transmembrane helices (TM) joined by four small hydrophilic loops and three large loops. One large cytosolic loop (Loop 6) in Scap binds COPII proteins. The other two large loops (Loops 1 and 7) face the ER lumen.

Previous studies localized the cholesterol-binding activity to the N-terminal membrane domain of Scap. Studies described in this thesis narrow down the cholesterol binding pocket to the first large luminal loop (Loop 1). Mutational analysis further suggests a direct interaction between luminal Loop 1 and Loop 7 to control Scap transport activity.

Scap Loop 1 was purified as a recombinant protein and found to bind [³H]-cholesterol through an *in vitro* binding assay. The specificity of this binding was determined through competition studies with different unlabeled sterols. Importantly, the binding affinity and specificity of Loop 1 was similar to that of the entire Scap membrane domain.

Subsequently, alanine scan mutagenesis was performed on luminal Loop1 and Loop7. Through this approach, two point mutations of Scap (Y234A in Loop 1 and Y640S in Loop 7) were identified that prevent its movement to the Golgi, thus abrogating the processing of SREBPs. Trypsin cleavage assays on the full-length Scap show that Loop 6 of Scap(Y234A) or Scap(Y640S) is always in the configuration that precludes COPII binding, even in sterol-depleted cells.

When the Scap TM1-6 segment (containing Loop 1) and the TM7-end segment (containing Loop 7) are expressed in the same cells, the two proteins bind to each other as determined by co-immunoprecipitation. This binding does not occur when Loop 1 contains the Y234A mutation, or Loop 7 contains the Y640S mutation. These data support the model that luminal Loop 1 and luminal Loop 7 must interact in order for Scap movement to occur.

ACKNOWLEDGEMENTS

I thank Dr. Michael Brown and Dr. Joseph Goldstein, for the opportunity to learn experimental biology. Coming from a computational biology background, experimental biology required a big adjustment. They are patient and supportive. I have a better understanding of what science is and how to design a control experiment and evaluate the results.

I also thank my thesis committee members Drs. Philip Thomas, Joachim Seemann, and Michael Roth for useful suggestions and help.

I would like to acknowledge members of the Brown and Goldstein group who have invested time to teach me science- Michael Wang, Massoud Motamed, Arun Radhakrishnan. Massoud Motamed was of great guidance and taught me how to make progress. I would also like to thank my colleagues Kwang Min Lee, Akash Das, Nick Grishin, Lisa Kinch, Dan Rosenbaum, and Jin Ye for helpful comments. Additionally, I would like to thank Dorothy Williams for excellent technical assistance, and Lisa Beatty, Muleya Kapaale, and Ijeoma Dukes for invaluable help with tissue culture.

My family has been a great encouragement for me. My parents and wife have understood the importance of the time I have invested in the lab. My wife and son have provided me with a lot of happiness and joy, even when science isn't working well.

I would like to thank the support from Mechanisms of Disease and Translational Science Track at UT Southwestern and the HHMI Med into Grad Initiative.

TABLE OF CONTENTS

Abstract	v
Acknowledgements	vii
Table of Contents	viii
Prior Publications	ix
List of Figures	x
List of Abbreviations	xii
Chapter 1 – Introduction to SREBP Pathway and Scap Protein	1
Chapter 2 – Identification of Luminal Loop 1 of Scap Protein as the Sterol Sensor that Maintains Cholesterol Homeostasis	
Summary	4
Introduction	6
Experimental Procedures	8
Results	14
Figures	21
Discussion	37
Chapter 3 – Point Mutation in Luminal Loop 7 of Scap Protein Blocks Interaction with Loop 1 and Abolishes Movement to Golgi	
Summary	41
Introduction	43
Experimental Procedures	44
Results	48
Figures	55
Discussion	69
Chapter 4 – Conclusion and Perspective	71
Bibliography	75

PRIOR PUBLICATIONS

Zhang Y, Motamed M, Seemann J, Brown MS, Goldstein JL. Point mutation in luminal loop 7 of Scap protein blocks interaction with loop 1 and abolishes movement to Golgi. J Biol Chem. 2013 May 17; 288(20):14059-67.

Motamed M, **Zhang Y**, Wang ML, Seemann J, Kwon HJ, Goldstein JL, Brown MS. Identification of luminal loop 1 of Scap protein as the sterol sensor that maintains cholesterol homeostasis. J Biol Chem. 2011 May 20; 286(20):18002-12.

Li D*, **Zhang Y***, Xu L*, Zhou L, Wang Y, Xue B, Wen Z, Li P, Sang J. Regulation of gene expression by FSP27 in white and brown adipose tissue. BMC Genomics. 2010 Jul 22; 11:446.
(*Equal contribution)

Li JZ, Lei Y, Wang Y, **Zhang Y**, Ye J, Xia X, Pan X, Li P. Control of cholesterol biosynthesis, uptake and storage in hepatocytes by Cideb. Biochim Biophys Acta. 2010 May; 1801(5):577-86.

Toh SY, Gong J, Du G, Li JZ, Yang S, Ye J, Yao H, **Zhang Y**, Xue B, Li Q, Yang H, Wen Z, Li P. Up-regulation of mitochondrial activity and acquirement of brown adipose tissue-like property in the white adipose tissue of fsp27 deficient mice. PLoS One. 2008 Aug 6; 3(8):e2890.

Wu C*, **Zhang Y***, Sun Z, Li P. Molecular evolution of Cide family proteins: novel domain formation in early vertebrates and the subsequent divergence. BMC Evol Biol. 2008 May 23; 8:159. (*Equal contribution)

LIST OF FIGURES

CHAPTER 1

FIGURE 1-1: SREBP Pathway.....	1
FIGURE 1-2: SCAP Membrane Region.....	3

CHAPTER 2

FIGURE 2-1: Topology Model of the Membrane Region of Hamster Scap, Showing its three Functional Domains	21
FIGURE 2-2: Biochemical Properties of His ₆ -Scap(Loop1)	23
FIGURE 2-3: [³ H]Sterol Binding to His ₆ -Scap(Loop1).....	25
FIGURE 2-4: Association and Dissociation of [³ H]Cholesterol Binding to His ₆ -Scap(Loop1).....	26
FIGURE 2-5: Comparison of the Sterol Specificity of [³ H]Cholesterol Binding to Scap(Loop1) and Scap(TM1-8)	27
FIGURE 2-6: Alanine Scan Mutagenesis of Loop 1 region of Hamster Scap.....	29
FIGURE 2-7: ER-to-Golgi Transport of WT and Y234A Mutant Version of GFP-Scap.....	31
FIGURE 2-8: Biochemical Characterization of the Y234A Mutant Scap	33
FIGURE 2-9: Cycloheximide-Mediated Decline in Transfected WT and Y234A Mutant Version of GFP-Scap in CHO Cells.....	36

CHAPTER 3

FIGURE 3-1: Topology Model of the Membrane Domain of Hamster Scap, Showing its three Functional Domains and the sites of three Point Mutations (Y234A, D428A, and Y640S) that Confer a Constitutive Cholesterol-Bound Conformation, even in the Absence of Sterols.....	55
---	----

FIGURE 3-2: Alanine-Scanning Mutagenesis of Loop 7 region of Hamster Scap	57
FIGURE 3-3: Immunoblot Analysis of SREBP-2 Cleavage in Scap-Deficient Cells Transfected with WT or Y640S mutant version of full-length Scap in the Absence or Presence of transfected Insig-1	60
FIGURE 3-4: Biochemical Characterization of Y640S Scap	62
FIGURE 3-5: Mutant GFP-Scap (Y640S), but not WT GFP-Scap, fails to reach the Golgi	65
FIGURE 3-6: Co-Immunoprecipitation of NH ₂ - and COOH-terminal Segments of WT Scap, but not mutant Scap(Y640S)	67

LIST OF ABBREVIATIONS

bHLH-Zip, basic helix-loop-helix–leucine zipper

CHO, Chinese hamster ovary

CMV, cytomegalovirus

COPII, coat protein complex II

DMEM, Dulbecco's modified Eagle's medium

DTT, dithiothreitol

Endo H, endoglycosidase H

ER, endoplasmic reticulum

FCS, fetal calf serum

GFP, Green Fluorescent Protein

HMG CoA, 3-hydroxy-3-methylglutaryl-coenzyme A

HSV, herpes simplex virus

LDL, low density lipoprotein

Ni-NTA, nickel-nitrilotriacetic acid

NP-40, nonidet P-40

NPC1, Niemann-Pick Type C1 disease protein

PBS, phosphate-buffered saline

PNGase F, Peptide: N-Glycosidase F

Scap, SREBP cleavage-activating protein

SRE, sterol regulatory element

SREBP, sterol regulatory element-binding protein

TK, thymidine kinase

TM, transmembrane helices

WT, wild-type

25-HC, 25-hydroxycholesterol

CHAPTER ONE

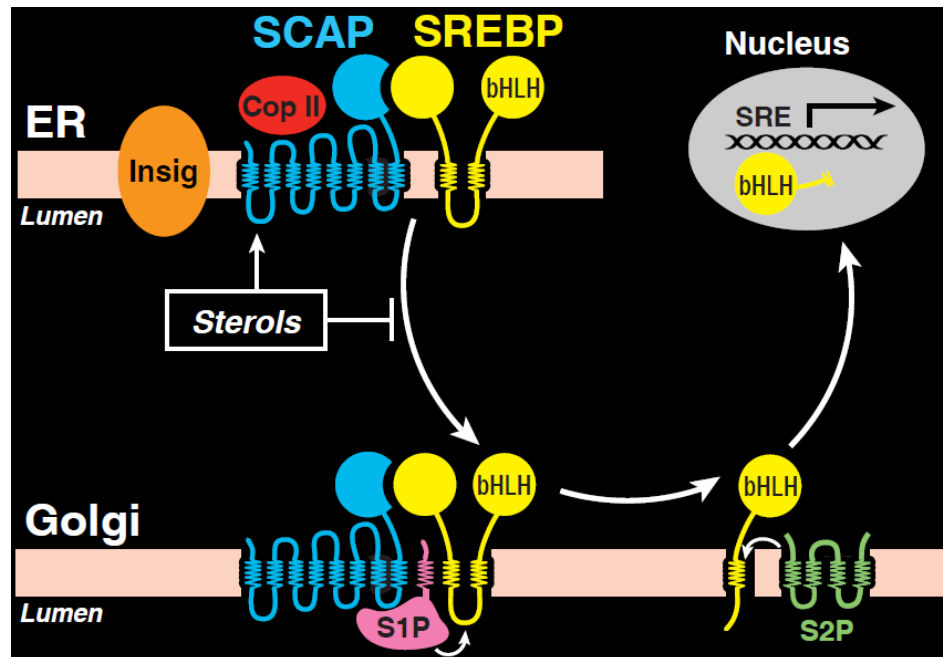
INTRODUCTION TO SREBP PATHWAY AND SCAP PROTEIN

THE SREBP PATHWAY

Lipid homeostasis in animal cells is controlled by a basic helix-loop-helix–leucine zipper (bHLH-Zip) family of transcription factors called sterol regulatory element (SRE)-binding proteins (SREBPs) (Brown and Goldstein, 1997). SREBPs directly activate all of the genes necessary to produce cholesterol, fatty acids, and triglycerides (Horton et al., 2002). Unlike other bHLH-Zip transcription factors, the SREBPs are synthesized as intrinsic transmembrane proteins of the endoplasmic reticulum (ER). Immediately after synthesis, the SREBPs form a complex with a membrane-embedded escort protein called SCAP. In lipid-depleted cells, SCAP facilitates the incorporation of SREBPs into COPII-coated vesicles that bud from the ER and travel to the Golgi apparatus, where the SREBPs are processed sequentially by two membrane-bound proteases S1P and S2P. Subsequent release of SREBPs transcription factor domain facilitates entry into the nucleus and activation of the genes encoding enzymes required for synthesis of cholesterol and fatty acids. When cholesterol accumulates in ER membranes, SCAP undergoes a conformational change that causes it to bind to Insig, an ER retention protein. This binding prevents SCAP from escorting SREBPs to the Golgi, thereby abrogating the proteolytic processing of SREBPs. This feedback inhibition is essential to the prevention of cholesterol overproduction in animals (Goldstein et al., 2006).

FIGURE 1-1. SREBP pathway.

FIGURE 1-1

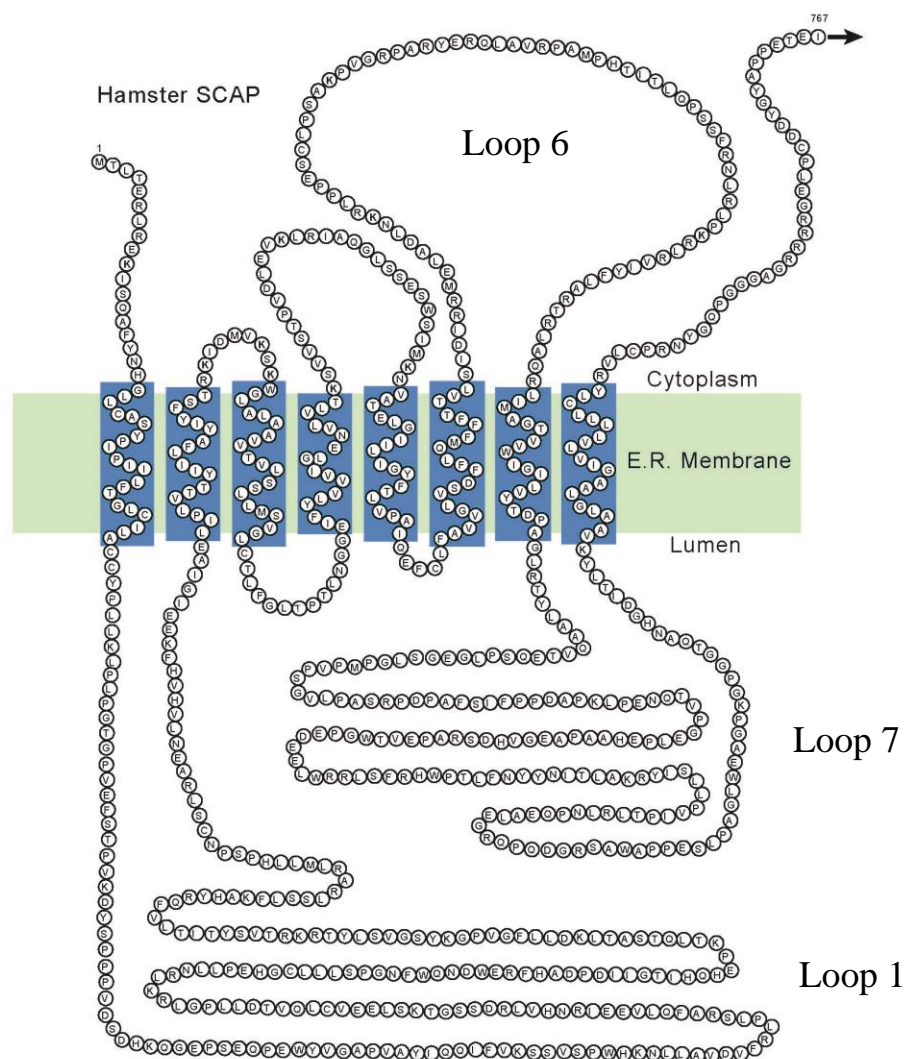


Scap

Scap has an N-terminal membrane attachment domain and a large C-terminal cytosolic domain that interacts with the regulatory domain of SREBP (Sakai et al., 1997). The Scap membrane region contains eight transmembrane helices (TM) connected by four small hydrophilic loops and three large loops (Nohturfft et al., 1998b). One large loop (Loop 6) faces the cytosol where it binds COPII proteins that initiate transport to the Golgi (Sun et al., 2005; Sun et al., 2007), and the other two large loops (Loops 1 and 7) are in the ER lumen with unknown function.

Scap is the cholesterol sensor. But the sterol sensing mechanism in Scap is not yet understood. It was previously postulated that an evolutionarily conserved segment which includes five of the eight membrane spanning helices of SCAP (TM 2-6) functions as the “sterol-sensing domain” (Hua et al., 1996; Nohturfft et al., 1998a). Mutations in this domain have been found to affect SCAP•Insig interactions (Feramisco et al., 2005; Yabe et al., 2002b).

FIGURE 1-2



CHAPTER TWO

IDENTIFICATION OF LUMINAL LOOP 1 OF SCAP PROTEIN AS THE STEROL SENSOR THAT MAINTAINS CHOLESTEROL HOMEOSTASIS

SUMMARY

Cellular cholesterol homeostasis is maintained by Scap, an endoplasmic reticulum (ER) protein with eight predicted transmembrane helices. In cholesterol-depleted cells, Scap transports Sterol Regulatory Element-binding Proteins (SREBPs) to the Golgi where the active fragment of SREBP is liberated by proteases so that it can activate genes for cholesterol synthesis. When ER cholesterol increases, Scap binds cholesterol, and this interaction changes the conformation of cytosolic Loop 6, which contains the binding site for COPII proteins. The altered conformation precludes COPII binding, abrogating movement to the Golgi. Consequently, cholesterol synthesis declines. Here, we identify the cholesterol-binding site on Scap as Loop 1, a 245-amino acid sequence that projects into the ER lumen. Recombinant Loop 1 binds sterols with a specificity identical to that of the entire Scap membrane domain. When tyrosine-234 in Loop 1 is mutated to alanine, Loop 6 assumes the cholesterol-bound conformation, even in sterol-depleted cells. As a result, full length Scap(Y234A) cannot mediate SREBP processing in transfected cells. These results indicate that luminal Loop 1 of Scap controls the conformation of cytosolic Loop 6, thereby determining whether cells produce cholesterol.

Material from Chapter 2 was originally published in Journal of Biological Chemistry. Motamed M, Zhang Y, Wang ML, Seemann J, Kwon HJ, Goldstein JL, Brown MS. Identification of Luminal Loop 1 of Scap Protein as the Sterol Sensor that Maintains Cholesterol Homeostasis. J Biol Chem. 2010 May 20; 286(20):18002-12.

INTRODUCTION

The endoplasmic reticulum (ER) protein Scap is unique in nature because it serves as a cholesterol sensor that assures the proper amount of cholesterol in membranes of animal cells (Radhakrishnan et al., 2007; Sun et al., 2007). The function of Scap derives from its ability to mediate the regulated transport of Sterol Regulatory Element-binding Proteins (SREBPs) from ER to Golgi. SREBPs are a family of three transcription factors that have the capacity to activate all of the genes necessary to produce cholesterol, fatty acids, and triglycerides (Horton et al., 2002). The SREBPs are synthesized as intrinsic transmembrane proteins of the ER. Immediately after their synthesis, the SREBPs bind to Scap, which serves as the nidus for incorporation into COPII-coated vesicles, which bud from the ER and travel to the Golgi. There the SREBPs are processed sequentially by two proteases, thereby releasing the active transcriptional fragments which travel to the nucleus. When cholesterol accumulates in ER membranes, Scap binds the cholesterol and undergoes a conformational change which causes it to bind to Insig, an ER resident protein (Goldstein et al., 2006). As a result of the conformational change and its stabilization by Insig (Gong et al., 2006), the Scap•SREBP complex is no longer incorporated into budding vesicles, and the active fragment cannot reach the nucleus. As a result, synthesis of cholesterol and fatty acids declines.

The 1276 amino acids of Scap can be divided into two functional regions (see Fig. 2-1). The COOH-terminal domain of ~540 amino acids extends into the cytosol. It contains four to seven WD repeat sequences that mediate its binding to SREBPs. The NH₂-terminal region of ~735 amino acids is the membrane attachment domain. It contains eight α -helices separated by hydrophilic loops (Nohturfft et al., 1998b). Three of the loops (Loops 1, 6, and 7) are long enough to have significant structure. Helices 2-6 contain the Insig binding site (Yabe et al.,

2002b; Yang et al., 2002). Loop 6, which faces the cytosol, contains the hexapeptide sequence MELADL which serves as the binding site for the COPII proteins that cluster the Scap•SREBP complex into COPII-coated vesicles that bud from ER membranes (Sun et al., 2005; Sun et al., 2007). When the cholesterol content of ER membranes exceeds a sharp threshold of 4-5% of total lipids, the cholesterol binds to the membrane region of Scap (Radhakrishnan et al., 2008), and this elicits a conformational change in Loop 6 that can be monitored by a protease protection assay (Brown et al., 2002). The change is reflected by the exposure of a novel arginine (Arg505) to cleavage by trypsin (Fig. 2-1).

The cholesterol-induced conformational change in Loop 6 causes the MELADL sequence to become inaccessible to COPII proteins, thereby precluding transport to the Golgi (Sun et al., 2007). Although the conformational change does not require Insig, binding to Insig stabilizes the inactive conformation, thereby lowering the threshold for cholesterol (Radhakrishnan et al., 2008).

Our previous cholesterol-binding studies were performed with a recombinant form of Scap that contained the entire membrane attachment domain (TM1-8) (Radhakrishnan et al., 2007; Radhakrishnan et al., 2004). Within this domain the precise site of cholesterol binding was not established. In the current study, we localize the cholesterol-binding site to Scap Loop 1, which faces the ER lumen. We show that a point mutation in Loop 1 elicits the same conformational change in Loop 6 that is created by cholesterol binding. As a result, Scap with this point mutation cannot move from ER to Golgi, even in cholesterol-depleted cells. These studies implicate an interplay between luminal Loop 1 and cytosolic Loop 6 of Scap as a control mechanism for the regulation of cholesterol metabolism in animal cells.

EXPERIMENTAL PROCEDURES

Reagents – We obtained [1,2,6,7-³H]cholesterol (100 Ci/mmol) and [26,27-³H]25-hydroxycholesterol (75 Ci/mmol) from American Radiolabeled Chemicals; 24,25-epoxycholesterol and 24(S)-hydroxycholesterol from Avanti Polar Lipids; all other sterols from Steraloids, Inc.; Nonidet P-40 (NP-40), FuGENE 6, and Complete Protease Inhibitor Cocktail from Roche Applied Sciences; Protease Inhibitor Cocktail Set III and mouse anti-HSV monoclonal antibody from Novagen; trypsin (type I from bovine pancreas), monoclonal anti-Green Fluorescent Protein (GFP), anti-c-Myc Affinity Gel, c-Myc peptide and cycloheximide from Sigma; peptide N-glycosidase (PNGase F) from New England Biolabs; Fos-choline 13 from Anatrace; Ni-NTA agarose beads from Qiagen; cyclodextrins from Trappsol; mouse anti-His monoclonal antibody, Superdex 200 10/300 GL, Mono Q 5/50 GL, and HisTrap HP columns from GE Healthcare Biosciences; Gel Filtration Standard from Bio-Rad; rat anti-*Drosophila* hsc72 (BiP) polyclonal antibody from Babraham Institute, Cambridge UK (Cat. No. BT-GB-1435); phRL-TK (encoding *Renilla luciferase* gene) and Dual-Luciferase Reporter Assay System from Promega; and bovine serum albumin (Cat. No. 23209) from Thermo Scientific. Complexes of methyl- β -cyclodextrin with cholesterol were prepared at a stock concentration of 2.5 mM (Brown et al., 2002). Newborn calf lipoprotein-deficient serum (d>1.215 g/ml) was prepared by ultracentrifugation (Goldstein et al., 1983). Solutions of compactin and sodium mevalonate were prepared as previously described (Brown et al., 1978; Kita et al., 1980). A stock solution of 10 mM sodium oleate-bovine serum albumin in 0.15 M NaCl (final pH 7.6) was prepared as previously described (Hannah et al., 2001). IgG-4H4, a mouse monoclonal antibody against hamster Scap (amino acids 1-767) (Ikeda et al., 2009) and IgG-9E10, a mouse monoclonal

antibody against c-Myc (Yabe et al., 2002a), were previously described in the indicated reference.

Buffers – Buffer A contained 50 mM Tris-chloride (pH 7.4), 150 mM NaCl, 1 mM dithiothreitol (DTT), and 0.005% (w/v) sodium azide. Buffer B contained 50 mM Tris-chloride (pH 7.4), 1 mM DTT, and 0.005% sodium azide. Buffer C contained 50 mM Tris-chloride (pH 7.4), 150 mM NaCl, and 0.004% NP-40. Buffer D contained 50 mM Tris-chloride (pH 7.4) and 150 mM NaCl. Buffer E contained 50 mM Tris-chloride (pH 7.5), 150 mM NaCl, 1 mM DTT, and 25 mM phosphocholine chloride. Buffer F contained 10 mM HEPES (pH 7.4), 10 mM KCl, 1.5 mM MgCl₂, 5 mM sodium EDTA, 5 mM sodium EGTA, and 250 mM sucrose. Buffer G contained 50 mM Tris-chloride (pH 7.4), 135 mM NaCl, 10 mM KCl, and 0.1% NP-40, and 1% (v/v) Protease Inhibitor Cocktail Set III.

Culture Medium – Medium A contained a 1:1 mixture of Ham's F-12 and Dulbecco's modified Eagle's medium supplemented with 100 units/ml penicillin and 100 µg/ml streptomycin sulfate. Medium B contained medium A supplemented with 5% newborn calf lipoprotein-deficient serum, 50 µM sodium mevalonate, and 50 µM compactin, and 1% (w/v) hydroxypropyl-β-cyclodextrin. Medium C contained medium A supplemented with 5% newborn calf lipoprotein-deficient serum, 50 µM sodium mevalonate, and 50 µM compactin. Medium D contained Dulbecco's modified Eagle's medium, low glucose (1000 mg/l) supplemented with 10% FCS and 100 units/ml penicillin and 100 µg/ml streptomycin sulfate.

Plasmids – The pFastBacHTa expression vector encoding amino acids 1-767 of hamster Scap, referred to as His₁₀-Scap(TM1-8) (Radhakrishnan et al., 2004), was modified by site-directed mutagenesis (QuikChange II XL kit, Stratagene) to generate a recombinant baculovirus designated pHis₆-Scap(Loop1). pHis₆-Scap(Loop1) encodes, in sequential order from the NH₂-

terminus, the signal sequence from honeybee mellitin (Tessier et al., 1991), an epitope tag consisting of 6 histidines, a TEV protease cleavage site (Kapust et al., 2002), and luminal Loop 1 of Scap (amino acids 46-269).

The following recombinant expression plasmids have been described: pCMV-Scap, encoding WT hamster Scap under control of cytomegalovirus (CMV) promoter (Sakai et al., 1997); pTK-Scap, encoding WT hamster Scap under control of thymidine kinase (TK) promoter; pGFP-Scap, encoding GFP fused to WT hamster Scap under control of the CMV promoter (Nohturfft et al., 2000); pTK-HSV-BP2, encoding WT HSV-tagged human SREBP-2 under control of the TK promoter (Feramisco et al., 2005); pTK-Insig-1-Myc, encoding WT human Insig-1 followed by six tandem copies of c-Myc epitope tag under control of TK promoter (Gong et al., 2006); pCMV-Insig1-Myc, encoding human Insig-1 followed by 6 tandem copies of a c-Myc epitope tag (Yabe et al., 2002b); and pSRE-Luc, encoding three tandem copies of Repeat 2 + Repeat 3 of the human LDL receptor promoter, the adenovirus E1b TATA box, and the *Firefly luciferase* gene (Hua et al., 1996). Point mutations in the above Scap plasmids were produced by site-directed mutagenesis. The coding regions of all mutated plasmids were sequenced.

Purification of His-Tagged Scap(Loop1) from Sf9 Cells – On day 0, 1-liter cultures of Sf9 cells (5×10^5 cells/ml) in Sf-900 II SFM insect medium (Invitrogen) were set up at 27 °C. On day 1, cells were infected with His₆-Scap(Loop1) baculovirus. On day 3, cells were harvested and washed once with phosphate-buffered saline (PBS). The cells were then flash-frozen with liquid nitrogen and stored at -80 °C. Each pellet was resuspended in 10 pellet volumes of buffer A containing 1% (w/v) Fos-choline 13 and one Complete Protease Inhibitor Cocktail tablet per 50 ml, rotated for 1 h at 4 °C, and centrifuged at $10^5 \times g$ for 1 h at 4 °C. The resulting supernatant was loaded onto a 1-ml or 5-ml HisTrap HP column equilibrated with 10 column volumes of

buffer A containing 0.1% Fos-choline 13, then washed sequentially with 10 column volumes of buffer A containing 0.1% Fos-choline 13 and 5 mM imidazole, followed by 25 mM imidazole. The protein was then eluted with 5 column volumes of the above buffer containing 250 mM imidazole. Protein rich fractions containing His₆-Scap(Loop1) were combined and concentrated with a Millipore Centrifugal Filter Unit (10 kDa MWCO) to 1 ml, and then diluted 40-fold in buffer B containing 0.1% Fos-choline 13. The resulting solution was applied to a 1-ml Mono Q column, and the protein was eluted with the above buffer containing 50 mM NaCl. The peak fractions containing His₆-Scap(Loop1) were combined, concentrated to 0.5 ml with a Millipore Centrifugal Filter Unit (10 kDa MWCO), and then applied to a Superdex 200 10/300 GL column. His₆-Scap(Loop1) was eluted with buffer B containing 0.1% Fos-choline 13 between 12.5 ml and 14.5 ml, after which these fractions were combined, stored at 4°C, and used for assays within 2 days.

[³H]Cholesterol-binding Assay – All operations were carried out at room temperature. Binding reactions were set up in microcentrifuge tubes. Each reaction, in a final volume of 100 µl of buffer C with 0.004% NP-40, contained 5 pmol (150 ng) of purified His₆-Scap(Loop1) (delivered in 1 µl of buffer B containing 0.1% Fos-choline 13; final concentration in assay, 0.001%), and the indicated concentration of [³H]sterol (delivered in 2 µl ethanol) in the absence or presence of competitor sterol (delivered in 1 µl ethanol). After incubation for 4 h at room temperature, each reaction was loaded onto a column packed with 0.3 ml of Ni-NTA agarose beads preequilibrated with 2 ml of buffer D. The columns were washed with 5 ml of buffer D, and then eluted with 1 ml of the same buffer containing 250 mM imidazole. Aliquots of the eluate (0.7 ml) were assayed for radioactivity in a liquid scintillation counter.

[³H]Cholesterol Dissociation Assay – [³H]Cholesterol was prebound to His₆-Scap(Loop1) under standard assay conditions with 150 nM [³H]cholesterol (see above) except that the assay was scaled up 40-fold. After incubation for 4 h at room temperature, the protein-bound [³H]cholesterol was eluted from the Ni-NTA agarose beads in 1 ml and then diluted to a final volume of 6 ml with buffer A containing 0.1% Fos-choline 13. For the dissociation assay, the 6-ml mixture containing [³H]cholesterol bound to His₆-Scap(Loop1) was divided into two aliquots of 3 ml, each of which received an addition of 24 ml of buffer C in the absence or presence of 11 μM unlabeled cholesterol. After incubation at room temperature for the indicated time, a 1-ml aliquot from each of the 27-ml sample was transferred to a tube containing 600 μl of Ni-NTA-agarose beads. After incubation for 3 min at 4 °C, the beads were centrifuged at 800xg for 1 min at room temperature, after which the supernatant was assayed for radioactivity.

Cell Culture and Transfection – SRD-13A cells, a Scap-deficient cell line derived from CHO-7 cells (Rawson et al., 1999), were grown in monolayer at 37 °C in 8-9% CO₂ in medium A supplemented with 5% FCS, 1 mM sodium mevalonate, 20 mM sodium oleate-albumin, and 5 μg/ml cholesterol. SV589 cells, a line of SV-40 immortalized human fibroblasts (Yamamoto et al., 1984), were grown in monolayer at 37°C in 5% CO₂ in medium D. Hamster CHO-K1 cells were grown in monolayer at 37°C and 8-9% CO₂ in medium A supplemented with 5% FCS.

Trypsin Cleavage Assay of Scap – This assay was carried out as previously described by (Brown et al., 2002) with modifications in the culture and transfection conditions. On day 0, SRD-13A cells were set up for experiments in 10 ml of medium A containing 5% FCS at a density of 8×10^5 cells per 100-mm dish. On day 2, cells were transfected with 1 μg of full length WT pCMV-Scap or its mutant Y234A version in 7 ml of medium A supplemented with 5% FCS; FuGENE 6 was used as the transfection agent. On day 3, the cells were washed once with PBS,

harvested for preparation of membranes, and subjected to the trypsin cleavage assay (Brown et al., 2002).

Assay for Scap•Insig Complex – SRD-13A cells were set up for experiments as described above under “Trypsin Cleavage Assay of Scap” except that the cells were plated in 60-mm dishes at a density of 3×10^5 cells per dish. On day 2, the cells were transfected with 0.1 μ g pCMV-Insig1-Myc and 1 μ g of either full length WT pCMV-Scap or its mutant Y234A version. On day 3, the cells were switched to cyclodextrin-containing medium B. After incubation at 37°C for 1 h, cells were washed twice with PBS and switched to medium C in the absence or presence of either 30 μ M cholesterol complexed with methyl- β -cyclodextrin or 1 μ g/ml 25-hydroxycholesterol (delivered in ethanol, final concentration of 0.1%). After incubation for 4 h, cells were washed twice with PBS and harvested. The pellets from three 60-mm dishes of transfected SRD-13A cells were solubilized in 1 ml of NP-40-containing buffer G, passed through a 22.5-gauge needle 15 times and rotated for 1.5 h at 4°C. All subsequent operations were carried out at 4 °C unless otherwise stated. The cell extracts were clarified by centrifugation at $10^5 \times g$ for 30 min. Anti-Myc beads (50 μ l) were added to the supernatant, followed by rotation for 16 h and centrifugation at $2000 \times g$ for 1 min. The pelleted beads containing the immune complexes were washed on the rotator with 1 ml of buffer G for 30 min, followed by three additional washes in buffer G for 10 min each. The washed beads were eluted in 100 μ l buffer G with 0.25 mg/ml c-Myc peptides by rotating for 1 h at room temperature. After centrifugation at $2000 \times g$ for 1 min, the supernatant was subjected to immunoblot analysis.

SREBP-2 Processing in Cultured Cells – SRD-13 cells were set up for experiments as described in the legend to Fig. 2-7A. After transfection and incubation with sterols, nuclear and

membrane fractions were prepared as previously described (Feramisco et al., 2005) and then subjected to immunoblot analysis.

Immunoblot Analysis – Samples for immunoblotting were resolved with to 10% or 13% SDS/PAGE or electrophoresis on 12% Tris-tricine gels, after which the proteins were transferred to nitrocellulose filters that were incubated with the following primary antibodies: 1 µg/ml mouse monoclonal anti-His, 1:500 dilution of a rat antiserum directed against *Drosophila* hsc72 (BiP), 1 µg/ml mouse monoclonal anti-Myc IgG-9E10, or 5 µg/ml mouse monoclonal anti-Scap IgG-4H4. Bound antibodies were visualized by chemiluminescence (SuperSignal West Pico Chemiluminescent Substrate, Thermo Scientific) using a 1:5000 dilution of anti-mouse IgG (Jackson ImmunoResearch Laboratories, Inc.) or anti-rat IgG (GE Healthcare) conjugated to horseradish peroxidase. The films were exposed to Phoenix Research Products Blue X-ray Film (F-BX810) at room temperature.

RESULTS

Fig. 2-1 shows the sequence and the predicted topology of the membrane domain of Scap as deduced from previous studies (Nohturfft et al., 1998b). This segment has 8 predicted transmembrane helices and 3 loops that are large enough to have secondary structure. Loop 1 comprises 245 amino acids and faces the lumen. It contains a site for *N*-linked glycosylation near its C-terminus. Loop 6, which faces the cytosol, was shown previously to contain the sequence MELADL, which is the binding site for COPII proteins that carry the Scap•SREBP complex from ER to Golgi (Sun et al., 2005; Sun et al., 2007). Loop 7, which faces the lumen, contains an epitope that allows immunodetection of a tryptic fragment that changes in response to a sterol-induced conformational change in the structure of Loop 6 (Brown et al., 2002; Sun et al., 2007).

We prepared a baculovirus encoding nearly the entire Loop 1 (residues 46-269) preceded by a cassette comprised of the signal sequence from honeybee mellitin followed by 6 histidines and a TEV protease cleavage site. After introduction into insect cells, the cells produced Loop 1 as a membrane-attached protein (Fig. 2-2A, *lanes 1, 2*). No detectable amounts of Loop 1 were secreted into the medium. Membrane-bound Loop 1 showed two bands upon SDS-PAGE. NH₂-terminal sequencing by Edman degradation revealed that the upper band represents protein that retains the signal sequence because it has not been cleaved by signal peptidase. The lower band contains protein that was processed by signal peptidase. Treatment with TEV protease reduced both proteins to a single band (data not shown). Both forms of the protein could be solubilized from the membrane by treatment with a detergent (Fos-choline 13) (Fig. 2-2A, *lanes 3, 4*), but neither one was released by treatment with Na₂CO₃ at pH 11 (Fig. 2-2A, *lanes 5, 6*), indicating that Loop 1 is attached to the membrane by hydrophobic forces. The detergent-solubilized protein was purified by sequential chromatography on a nickel agarose column and an ion exchange column, followed by gel filtration. Upon gel filtration in 0.1% Fos-choline 13, the protein had an apparent molecular mass of 125 kDa (Fig. 2-2B), consistent with a tetramer. Circular dichroism indicated a largely helical structure (Fig. 2-2C).

Sterol-binding studies were performed with preparations of purified Scap Loop 1 that contained molecules with and without the signal sequence. To measure cholesterol binding, we incubated the recombinant protein with [³H]cholesterol in buffer containing 0.004% NP-40 and 0.001% Fos-choline 13. The mixture was applied to a nickel agarose column that was washed without detergent, and the protein-bound [³H]cholesterol was eluted with 250 mM imidazole in detergent-free buffer and quantified by scintillation counting. As shown in Fig. 2-3, the recombinant Loop1 bound [³H]cholesterol with saturation kinetics (calculated K_d = 67 nM),

which is comparable to the apparent K_d of 50-100 nM when the binding studies were performed with the entire membrane attachment domain (TM1-8) (Radhakrishnan et al., 2004). The rate of dissociation of previously bound [3 H]cholesterol from Loop 1, as measured in the presence of an excess of unlabeled cholesterol, was similar to that previously shown for Scap(TM1-8), i.e., half-time of dissociation of ~10 min (Fig. 2-4 and see Fig. 4 from Radhakrishnan, *et al.*) (Radhakrishnan et al., 2004). Moreover, like the entire membrane domain of Scap, Loop 1 did not bind [3 H]25-hydroxycholesterol with high affinity (Fig. 2-3B).

To analyze the sterol specificity of Loop 1 binding, we performed competition studies with various unlabeled sterols. Androstenol and desmosterol competed as well as cholesterol for [3 H]cholesterol binding, whereas epicholesterol, lanosterol and 25-hydroxycholesterol did not compete (Fig. 2-5A). Fig. 2-5B compares the ability of various sterols at 1.5 μ M to compete for [3 H]cholesterol binding to Loop 1. For comparative purposes, Fig. 2-5C is reproduced from Fig. 3D of Radhakrishnan, *et al.*, (2007) (Radhakrishnan et al., 2007), who studied sterol competition for [3 H]cholesterol binding to the entire transmembrane region of Scap, designated Scap(TM1-8). The sterols are grouped into effective competitors (*shown in red*), partial competitors (*shown in blue*), and non-competitors (*shown in black*). The sterol specificity of Loop 1 coincides precisely with that of the entire transmembrane domain.

We next carried out alanine scan mutagenesis of Loop 1 to identify functional residues. Single residues or clusters of 2 or 3 contiguous residues were changed to alanine in a *Herpes simplex* TK vector that encodes full length Scap. The mutant plasmids were introduced into hamster SRD-13A cells, a mutant CHO cell line that lacks Scap (Rawson et al., 1999), together with plasmids encoding firefly luciferase under control of an SRE-containing promoter and

Insig-1 under control of the TK promoter. To control for transfection efficiency, we included a plasmid encoding *Renilla* luciferase under control of the TK promoter. The cells were depleted of cholesterol by incubation with hydroxypropyl- β -cyclodextrin, and some of the cells were replenished by addition of cholesterol complexed with methyl- β -cyclodextrin. The cells were harvested, and the ratio of firefly to *Renilla* luciferase was measured. In cells that received no Scap, there was little firefly luciferase activity (Fig. 2-6A). WT Scap led to high luciferase activity that was reduced by 80% in the presence of cholesterol. Several of the mutant plasmids showed no luciferase activity in the absence of cholesterol (indicated by red asterisks in Fig. 2-6A). We concluded that these mutations impaired the ability of Scap to carry SREBPs to the Golgi region.

To deconvolute the cluster mutations that appeared to abolish Scap activity, we prepared additional plasmids in which each of the residues in each cluster was changed individually to alanine (Fig. 2-6B). These data revealed two single amino acid substitutions that abolished Scap activity. These were V98A and Y234A. We chose the Y234A mutant for further study.

To visualize directly the lack of movement of Scap(Y234A) to the Golgi, we introduced the Y234A mutation into a plasmid encoding a fusion protein between Scap and green fluorescent protein (GFP) (Fig. 2-7). Cells were depleted of sterols and then fixed and permeabilized for fluorescence microscopy. Scap was visualized by its GFP tag. The Golgi complex was visualized by incubation with an antibody directed against Golgi protein GM130 followed by an anti-immunoglobulin coupled to a red Alexa dye. Nuclei were stained with Hoechst dye (blue). Under these conditions, WT Scap-GFP was concentrated in the Golgi where it co-localized with GM130 (*upper panels*, Fig. 2-7). In contrast, the vast majority of Scap(Y234A) was found in a lacy pattern corresponding to ER, and there was no specific localization to the Golgi (*bottom*

panels, Fig. 2-7). The images shown in Fig. 2-7 are representative of multiple transfected cells that were individually examined (n=79 WT and n=70 mutant).

To confirm that the Y234A mutation abolishes the ability of Scap to facilitate SREBP processing, we transfected plasmids encoding WT or Y234A mutant Scap into Scap-deficient SRD-13A cells (Fig. 2-8A). Some of the cells also received a plasmid encoding Myc-tagged Insig-1. The cells were depleted of sterols, and some were repleted with cholesterol or 25-HC. Nuclear extracts and membrane pellets were isolated and subjected to SDS/PAGE. In the absence of co-transfection with Insig-1, overexpression of WT Scap caused the appearance of the nuclear fragment of SREBP-2 (*lane 2*), and there was minimal reduction when cholesterol or 25-HC was added (*lanes 3 and 4*). When Insig-1 was overexpressed together with WT Scap, the nuclear fragment of SREBP-2 was seen in sterol-depleted cells (*lane 5*), and the fragment disappeared when cholesterol or 25-HC were present (*lanes 6 and 7*). When cells expressed Scap(Y234A), nuclear SREBP-2 was barely detectable in the absence or presence of sterols, and Insig-1 had no further inhibitory effect (*lanes 8-13*). Immunoblotting with anti-Scap confirmed the equal expression of WT and Y234A mutant Scap after transfection (*lanes 2-13*, Scap immunoblot).

To learn the reason for the defective behavior of Scap(Y234A), we introduced the mutation into a baculovirus encoding His-tagged Scap(Loop1), and we purified the mutant loop together with WT Loop 1 as described above. Both mutant and WT Loop 1 bound [³H]cholesterol with similar affinity (Fig. 2-8B). Fig. 2-8C shows the trypsin cleavage assay that we used previously to demonstrate a sterol-induced conformational change in Loop 6 of Scap (Brown et al., 2002; Sun et al., 2007) (see Fig. 2-1). Cells were transfected with plasmids encoding full-length WT Scap or the Y234A mutant. A 20,000xg pellet of sealed vesicles was isolated and incubated with

or without cholesterol complexed to methyl- β -cyclodextrin. The membranes were then treated with trypsin, after which the proteins were subjected to Tris-tricine gel electrophoresis and blotted with an antibody against an epitope in Loop 7 that faces the lumen and is thus protected from trypsin (see Fig. 2-1). In sterol-depleted membranes, trypsin cleaves Loop 6 at arginine 496 and arginines 747-750, which produces a fragment of 250 amino acids that corresponds to the band seen in Fig. 2-8C, *lane 1*. After incubation with cholesterol, arginines 503 and 505 become exposed to trypsin. Cleavage at these sites produces a fragment of ~241 amino acids, which corresponds to the lower band (*lane 3*). The Y234A mutant of Scap showed substantial amounts of the lower band, even in cholesterol-depleted membranes (*lane 2*). There was a further reduction in the upper band when cholesterol was added (*lane 4*). These data indicate that Loop 6 in the Y234A mutant is largely in the cholesterol-bound conformation even in sterol-depleted membranes.

When Scap is in the cholesterol-bound conformation, the protein binds to Insig, which stabilizes the cholesterol-bound conformation (Yang et al., 2002). Fig. 2-8D shows an experiment designed to determine whether Scap(Y234A) binds to Insig-1 in sterol-depleted cells as determined by an Insig-1 co-immunoprecipitation assay. Scap-deficient SRD-13A cells were co-transfected with plasmids encoding Myc-tagged Insig-1 and either WT Scap or the Y234A mutant. The cells were depleted of cholesterol, and some were repleted with cholesterol or 25-HC. Detergent extracts were prepared, and Insig-1 was precipitated with anti-Myc. After SDS-PAGE, the precipitates were probed with antibodies against Scap and Insig-1. In sterol-depleted cells, WT Scap did not co-precipitate with Insig-1 (Fig. 2-8D, *lane 1*). Addition of cholesterol (*lane 2*) or 25-HC (*lane 3*) caused Scap to be co-precipitated. In contrast, Scap(Y234A) was co-precipitated with Insig-1 even in the absence of sterol (*lane 4*), and the amount co-precipitated

increased when 25-HC was added (*lane 6*). In the immunoblots in this experiment, we noted that Scap showed two bands. We believe that the upper band represents an SDS-resistant dimer that forms when Scap has been incubated in detergents for prolonged periods, as required for the co-immunoprecipitation experiment. Insig-1 also appears as a doublet owing to the presence of two initiator methionines (Yang et al., 2002).

FIGURE 2-1. Topology model of the membrane region of hamster Scap, showing its three functional domains.

The cholesterol-binding domain is localized to luminal Loop 1; the three hydrophobic patches in its amino acid sequence are shaded in yellow, and the *N*-linked glycosylation site is denoted by the red box. The Insig-binding domain is localized to transmembrane helices 2-6, shown by the blue bracket. The COPII-binding site is localized to the MELADL sequence in Loop 6, shaded in red. Amino acids 496-747/750 (shaded in purple) correspond to the trypsin-resistant fragment generated by a sterol-regulated conformational change in Scap.

FIGURE 2-1

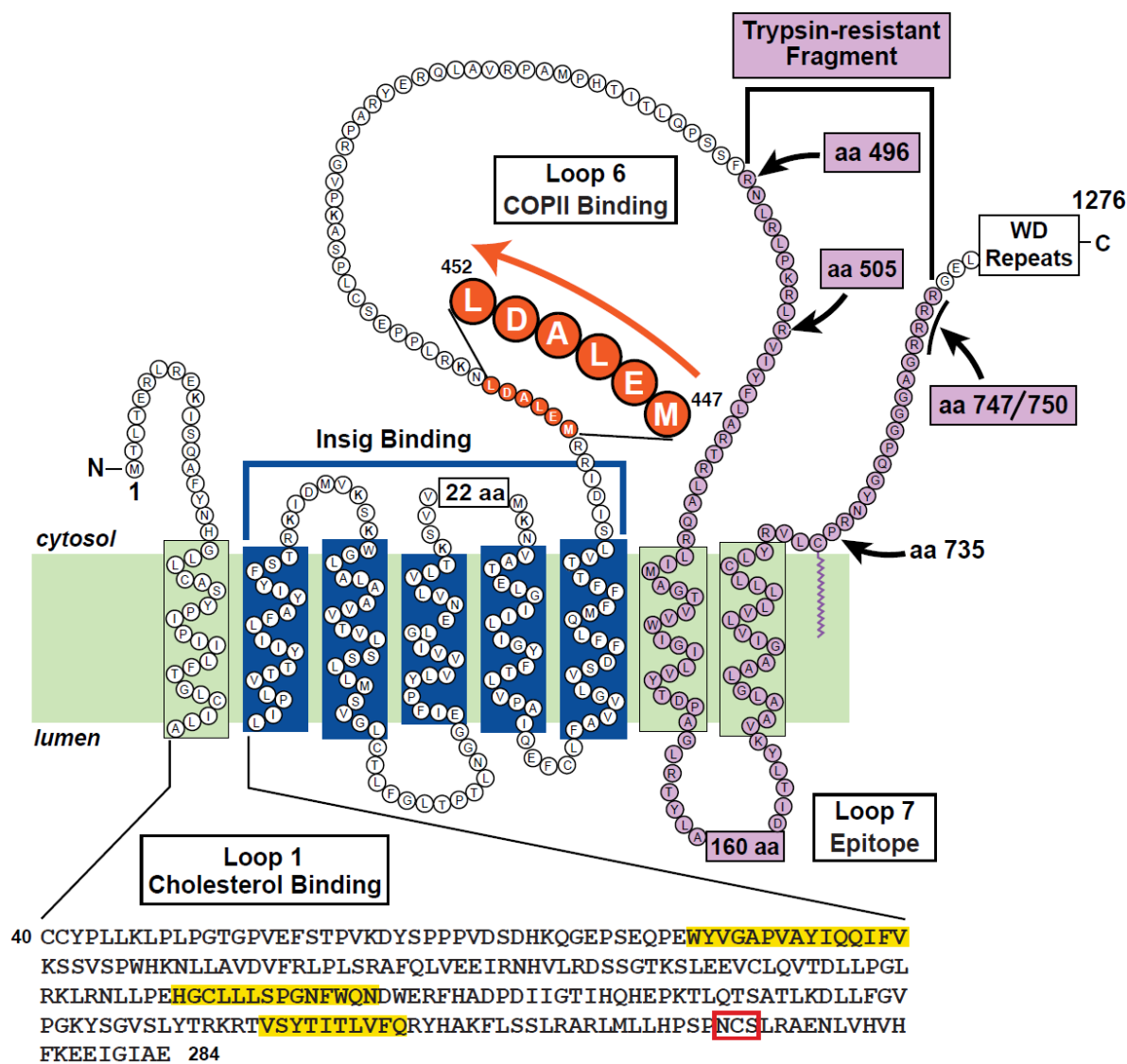


FIGURE 2-2. Biochemical properties of His₆-Scap(Loop1).

A, membrane attachment. Aliquots of baculovirus-infected Sf9 cell pellets (representing $\sim 2 \times 10^5$ cells) were each homogenized in 0.5 ml of one of the following buffers: 50 mM Tris-chloride (pH 7.4) and 100 mM NaCl (*lanes 1, 2*); buffer A with 1% Fos-choline 13 (*lanes 3, 4*); or 100 mM sodium carbonate at pH 11 (*lanes 5, 6*). After rotating for 2 h at 4 °C, the samples were centrifuged at $10^5 \times g$ for 30 min at 4 °C, after which the resulting pellets were solubilized in 0.5 ml of 10 mM Tris at pH 7.4, 100 mM NaCl, and 1% SDS. Aliquots of the supernatant (S) and pellet (P) were subjected to 13% SDS/PAGE and immunoblot analysis with anti-His (Scap(Loop1)) or anti-BiP. Films were exposed for 8-10 sec. *B*, molecular weight determination. Buffer A containing 0.1% Fos-choline 13 and either gel filtration standards or 125 μ g of His₆-Scap(Loop1) were loaded in a final volume of 0.5 ml onto a Superdex 200 10/300 GL column and chromatographed at a flow rate of 0.5 ml/min. Elution volumes for the gel filtration standards and for His₆-Scap(Loop1) were identified by monitoring absorbance at 280 nM and immunoblotting with anti-His, respectively. *C*, circular dichroism spectroscopy. Spectroscopic measurements of 3 μ M His₆-Scap(Loop1) in buffer A containing 0.1% Fos-choline 13 were carried out in an Aviv 62DS spectrometer using a 2-mm path length cuvette. The mean of 4 spectra for each curve is shown.

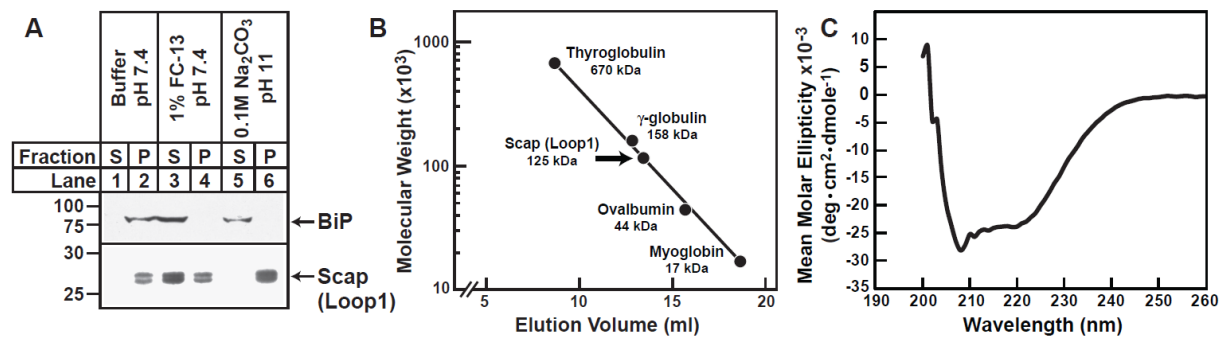
Figure 2-2

FIGURE 2-3. [^3H]Sterol binding to His₆-Scap(Loop1).

Each reaction, in a final volume of 100 μl buffer C with 0.004% NP-40 and 0.001 Foscholine-13, contained 5 pmol of purified His₆-SCAP(Loop1), 1 μg bovine serum albumin, and the indicated concentration of either [^3H]cholesterol (222 dpm/fmol) or [^3H]25-hydroxycholesterol (165 dpm/fmol) in the absence (\bullet) or presence (\circ) of 10 μM unlabeled sterol as indicated. After 4 h at room temperature, the bound [^3H]sterol was measured as described in *Experimental Procedures*. Each data point denotes the mean \pm SEM of triplicate assays. A, total [^3H]cholesterol binding without subtraction of blank values. B, specific [^3H]cholesterol or [^3H]25-hydroxycholesterol binding after subtraction of blank values determined in the presence of the respective unlabeled sterol at 10 μM (<127 fmol/tube for [^3H]cholesterol binding; <30 fmol/tube for [^3H]25-hydroxycholesterol binding).

Figure 2-3

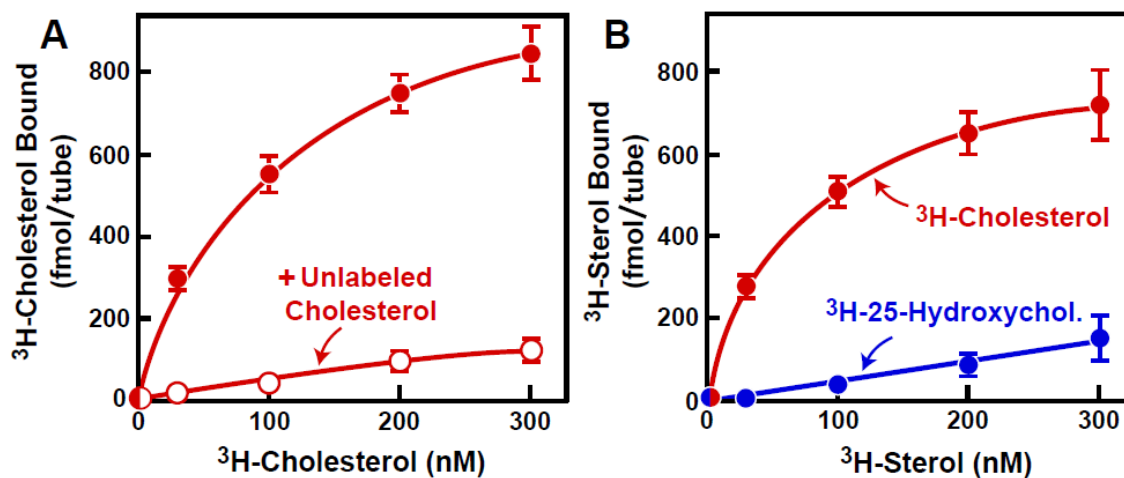


FIGURE 2-4. Association and dissociation of [^3H]cholesterol binding to His₆-Scap(Loop1).

A, time course of binding of [^3H]cholesterol to His₆-Scap(Loop1). Each reaction, in a final volume of 100 μl of buffer C with 0.004% NP-40 and 0.001% Fos-choline 13, contained 5 pmol of His₆-Scap(Loop1), 1 μg bovine serum albumin, and 150 nM [^3H]cholesterol (222×10^3 dpm/pmol). After incubation for the indicated time at room temperature, bound [^3H]cholesterol was determined. Each value is the average of duplicate assays. Blank values obtained in parallel assays of tubes containing no protein (<7 fmol/tube) were subtracted from each data point. *B*, dissociation of previously bound [^3H]cholesterol from His₆-Scap(Loop1). Dissociation was measured as described in *Experimental Procedures*. Each value is the average of duplicate assays and represents the percentage of [^3H]cholesterol remaining bound relative to the zero-time value, which is designated as 100%. The zero-time values were 300 and 230 fmol/tube in the absence and presence of unlabeled cholesterol, respectively.

Figure 2-4

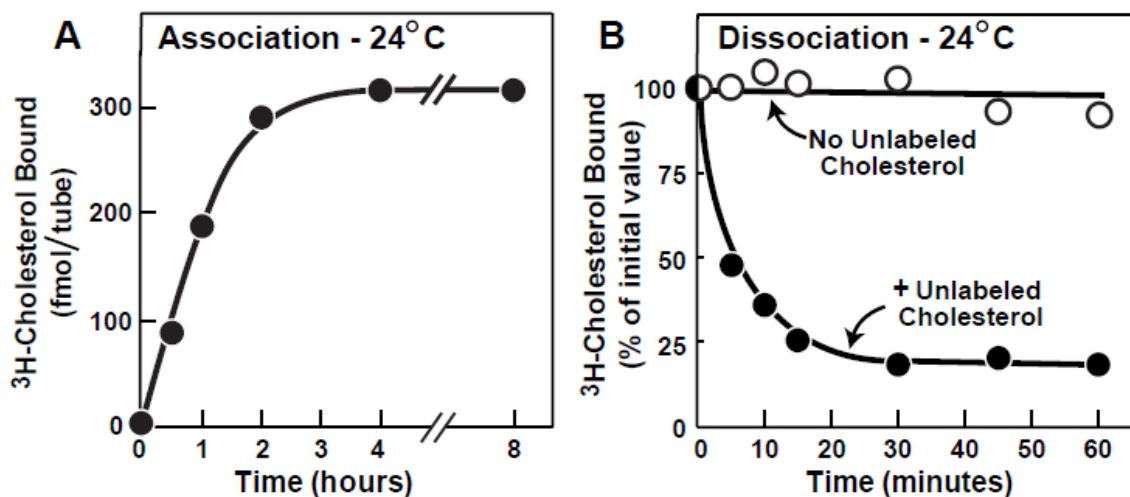


FIGURE 2-5. Comparison of the sterol specificity of [³H]cholesterol binding to Scap(Loop1) and Scap(TM1-8).

A and *B*, competitive binding of unlabeled sterols to His₆-Scap(Loop1). Each reaction, in a final volume of 100 µl of buffer C with 0.004% NP-40 and 0.001% Fos-choline 13, contained 5 pmol of His₆-Scap(Loop1), 1 µg bovine serum albumin, 150 nM [³H]cholesterol (222 dpm/fmol), and either varying concentrations of the indicated unlabeled sterol (*A*) or 1.5 µM of the indicated unlabeled sterol (*B*). After 4 h at room temperature, bound [³H]cholesterol was measured by the Ni-NTA agarose assay as described in *Experimental Procedures*. Each value represents total binding without subtraction of blank values and is the average of duplicate (*A*) or triplicate (*B*) assays. The “100% of control” values, determined in the absence of unlabeled sterols, was 398 fmol/tube and 673 fmol/tube in *A* and *B*, respectively. *C*, competitive binding of unlabeled sterols to His₁₀-Scap(TM1-8). These data are replotted from Fig. 3D of (Radhakrishnan et al., 2007). Briefly, each assay tube, in a final volume of 100 µl of buffer E with 0.1% Fos-choline 13, contained 120 nM His₁₀-Scap(TM1-8), 100 nM [³H]cholesterol (120 dpm/fmol), and 5 µM of the indicated sterol. After 4 h at room temperature, the amount of bound [³H]cholesterol was determined by the Ni-NTA agarose assay. The “100% of control” values, determined in the absence of unlabeled sterols, ranged from 209-263 fmol/tube. No blank values were subtracted. Each data point is the average of duplicate assays.

Figure 2-5

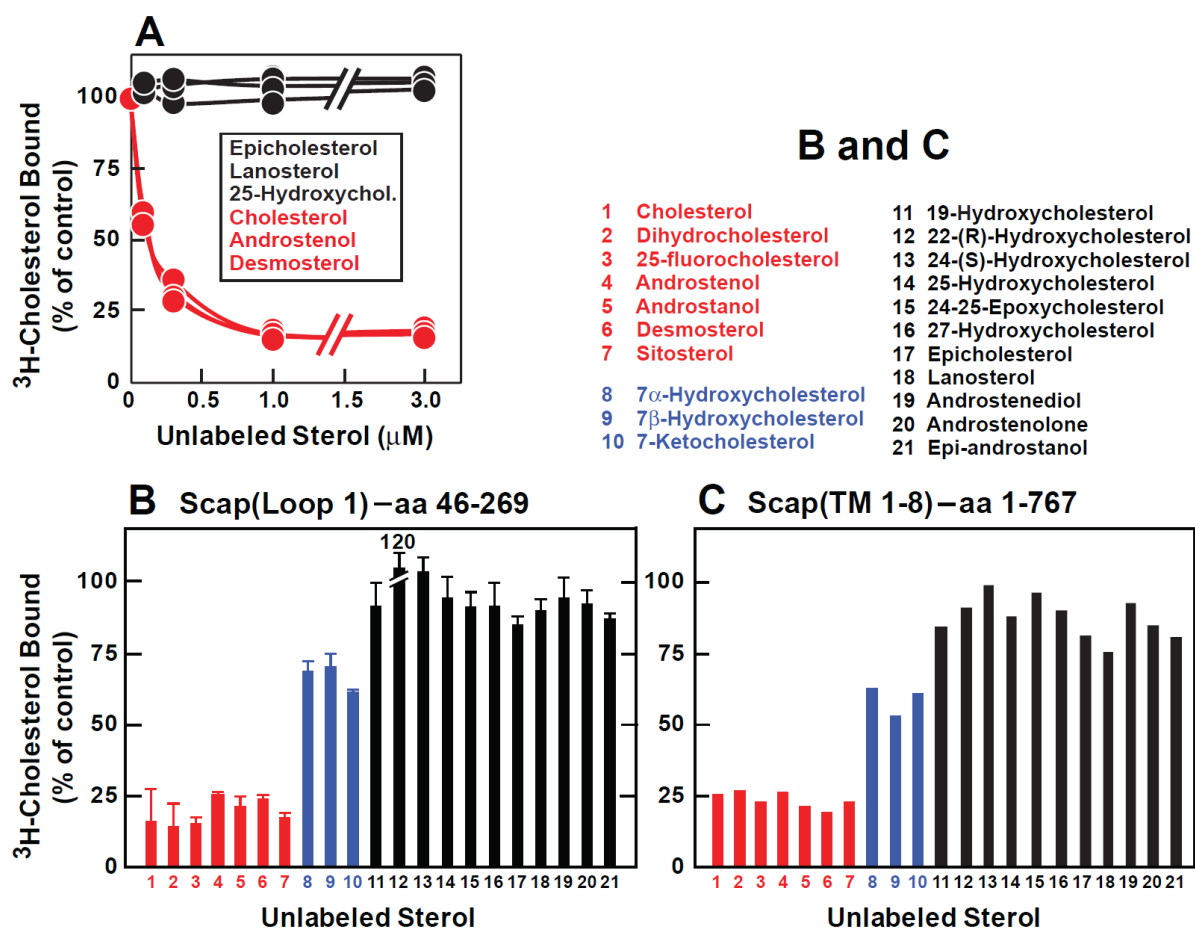


FIGURE 2-6. Alanine scan mutagenesis of Loop 1 region of hamster Scap.

A, B, on day 0, SRD-13 cells were set up for experiments in 1 ml of medium A containing 5% FCS at a density of 3×10^4 cells per well in 24-well plates. On day 1, cells in 1 ml of medium A supplemented with 5% FCS were cotransfected with 38 ng of pTK-Insig1-Myc, 125 ng pSRE-Firefly-Luciferase, 125 ng of pTK-*Renilla* luciferase, and 50 ng of WT pTK-Scap or the indicated mutant pTK-Scap in which 1 to 3 residues were mutated to alanine. FuGENE 6 was used as the transfection agent. For each transfection, the total amount of DNA was adjusted to 338 ng/dish by addition of pDNA3 mock vector. On day 2 (after incubation with plasmids for 24 h), the cells were washed once with PBS and then treated with hydroxypropyl- β -cyclodextrin-containing medium B for 1 h. Cells were then washed twice with PBS and refed with 1 ml of medium C in the absence or presence of 15 μ M cholesterol complexed with methyl- β -cyclodextrin. After incubation for 16 h, the cells were washed with PBS, after which luciferase activity was read on a Synergy 4 plate reader (BioTek) according to the Promega protocol. The amount of SRE-firefly luciferase activity in each dish was normalized to the amount of *Renilla* luciferase activity in the same dish. “Relative SRE-luciferase Activity” of 1.0 represents the normalized luciferase value in dishes transfected with WT pTK-Scap in the absence of cholesterol. All values are the average of duplicate assays. A, red asterisks denote single, double, or triple contiguous alanine mutations that produced a loss of SRE-luciferase activity in both the absence and presence of cholesterol. The data in these graphs were obtained in 4 different experiments, each with its own WT control. B, deconvolution of double or triple mutants that showed loss of SRE-luciferase activity in A. Red boxes denote single alanine mutations that continued to show loss of SRE-luciferase activity. Each value is the average of duplicate assays.

Figure 2-6

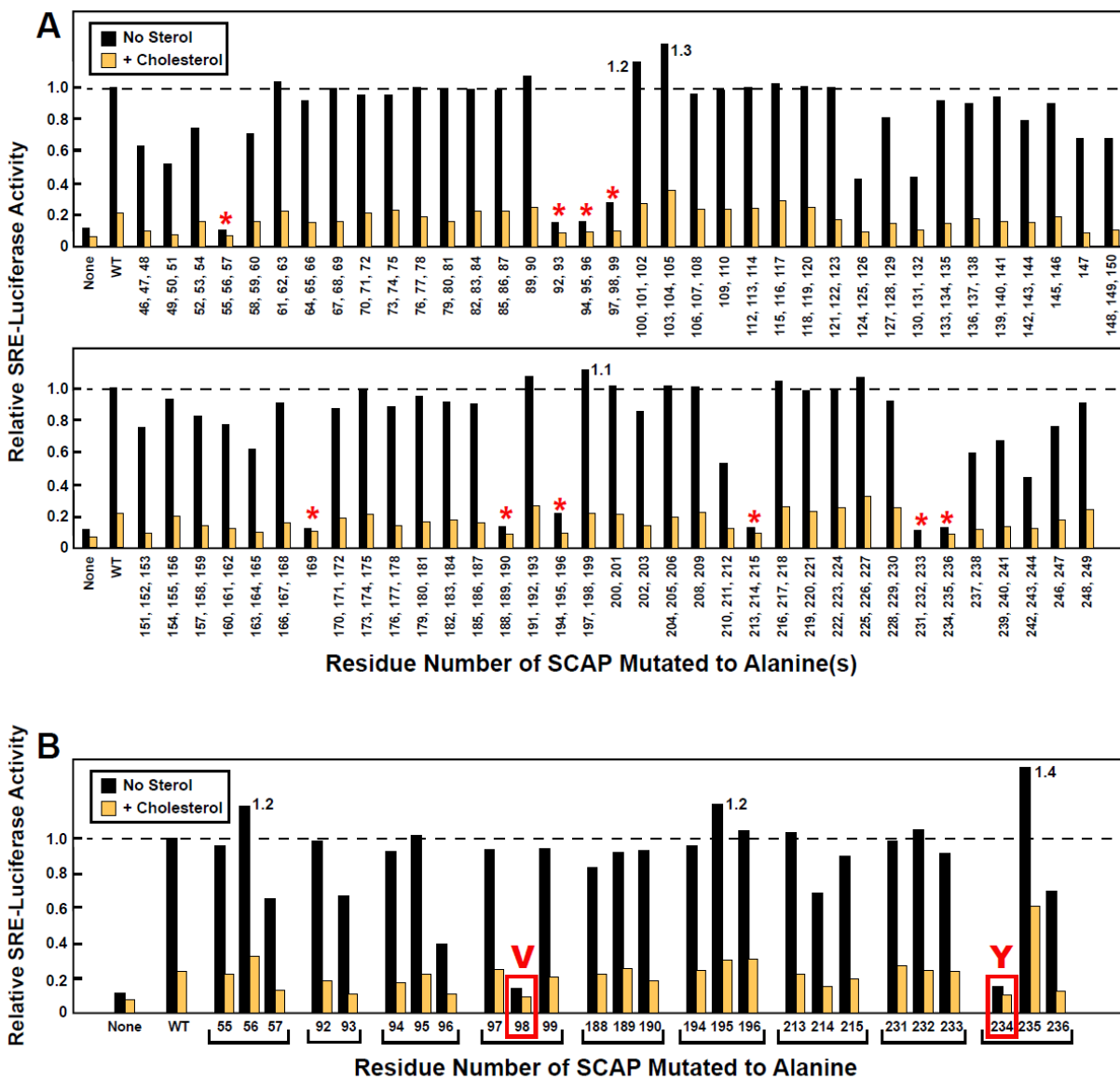


FIGURE 2-7. ER-to-Golgi transport of WT and Y234A mutant version of GFP-Scap.

On day 0, SV589 cells were set up for experiments in medium D at a density of 1×10^5 cells per 37-mm dish containing three 12-mm glass coverslips. On day 1, cells were transfected with 1 μ g of full length WT pGFP-Scap (*top panels*) or its mutant Y234A version (*bottom panels*) in 3 ml of medium A supplemented with 5% FCS. FuGENE 6 was used as the transfection reagent. On day 2, the cells were washed once with PBS and then incubated for 1 h at 37°C with cyclodextrin-containing medium B supplemented with 50 μ g/ml cycloheximide, after which each coverslip was fixed, permeabilized in methanol at -20 °C for 15 min, and then incubated with 0.625 μ g/ml of a monoclonal antibody against the Golgi resident protein GM130 (BD Biosciences) followed by 6.7 μ g/ml of goat anti-mouse antibodies conjugated to Alexa 594 (Invitrogen). The nuclei were then stained with 1 μ g/ml Hoechst 33342 (Invitrogen), and the coverslips were mounted in Mowiol 4-88 (Calbiochem) mounting solution (Wei and Seemann, 2009a). Fluorescence images were acquired using an LD Plan-Neofluar 40x/1.3 DIC objective, an Axiovert 200M microscope (Zeiss), an Orca 285 camera (Hamamatsu) and the software Openlab 4.0.2 (Improvision). Scale bar, 10 μ m.

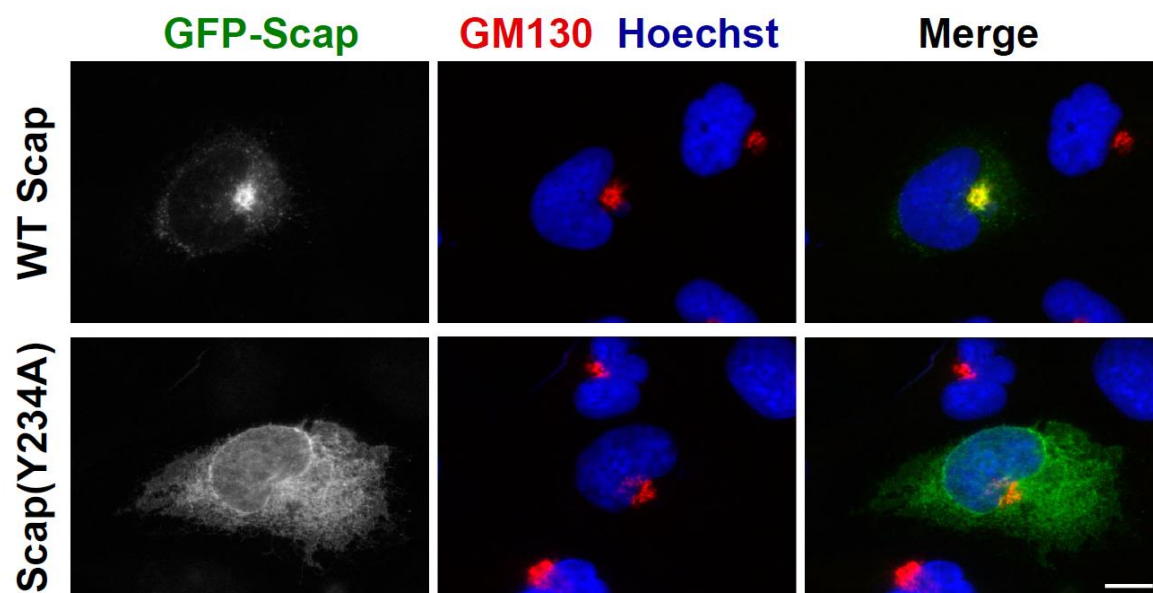
Figure 2-7

FIGURE 2-8. Biochemical characterization of the Y234A mutant Scap.

A, Immunoblot analysis of SREBP-2 in Scap-deficient cells transfected with WT or Y234A mutant version of full length Scap in the absence or presence of transfected Insig-1. On day 0, SRD-13A cells were set up for experiments at a density of 3×10^5 cells per 60-mm dish in 4 ml of medium A containing 5% FCS. On day 2, cells were transfected with 2 μ g TK-HSV-BP2 and 0.4 μ g of full length pTK-Scap (WT or its Y234A mutant) with or without 0.3 μ g of pTK-Insig 1-Myc in 7 ml of medium A supplemented with 5% FCS; FuGENE 6 was used as the transfection agent. For each transfection, the total amount of DNA was adjusted to 2.7 μ g/dish by addition of pDNA3 mock vector. On day 3, cells were washed once with PBS and then switched to hydroxypropyl- β -cyclodextrin-containing medium B for 1 h. The cells were washed with PBS and then incubated with medium C containing either 30 μ M cholesterol complexed with methyl- β -cyclodextrin or 1 μ g/ml 25-hydroxycholesterol (delivered in ethanol, final concentration of 0.1%) as indicated. After incubation for 4 h, the cells were harvested, and the isolated nuclear and membrane fractions were subjected to immunoblot analysis with 0.2 μ g/ml anti-HSV (SREBP-2), 5 μ g/ml IgG-4H4 (Scap), or 1 μ g/ml anti-Myc IgG-9E10 (Insig). Films were exposed for 8 to 20 sec. B, [3 H]cholesterol binding to WT and Y234A mutant version of His₆-Scap(Loop1). Each reaction, in a final volume of 100 μ l buffer C with 0.004% NP-40 and 0.001% Fos-choline 13, contained 5 pmol of purified WT and Y234A mutant version of His₆-Scap(Loop1), 1 μ g bovine serum albumin, and the indicated concentration of [3 H]cholesterol (222×10^3 dpm/pmol) in the absence or presence of 10 μ M unlabeled cholesterol. After 4 h at room temperature, the bound [3 H]cholesterol was measured as described in *Experimental Procedures*. Each data point is the average of duplicate assays and represents specific binding after subtraction of blank values determined in the presence of unlabeled cholesterol. C, tryptic

digestion of WT and Y234A mutant version of full length Scap transfected into Scap-deficient hamster cells. SRD-13A cells were transfected with the indicated full length pCMV-Scap plasmid and harvested for preparation of membranes as described in *Experimental Procedures*. Aliquots of the 20,000xg membrane fractions (100 μ g) were incubated for 20 min at room temperature with 50 μ M cholesterol complexed with methyl- β -cyclodextrin, followed by sequential treatments with 14 μ g/ml trypsin (30 min at 30 $^{\circ}$ C) and 4000 U/ml PNGase F (4 h at 37 $^{\circ}$ C). The samples were then subjected to immunoblot analysis with 5 μ g/ml anti-Scap IgG-4H4. The film was exposed for 30 sec. *D*, immune detection of Scap•Insig-1 complexes. On day 2, SRD-13A cells were cotransfected with pCMV-Insig1-Myc together with either full length pCMV-Scap or its mutant Y234A version as indicated. On day 3, the cells were incubated for 1 h with 1% hydroxypropyl- β -cyclodextrin, after which they received fresh medium containing one of the following sterols: none (-), 30 μ M cholesterol complexed with methyl- β -cyclodextrin (Chol), or 1 μ g/ml 25-HC. After incubation at 37 $^{\circ}$ C for 4 h, each detergent-solubilized whole cell lysate was incubated with anti-Myc beads, followed by washing and elution with Myc peptide as described in *Experimental Procedures*. The eluates were subjected to immunoblot analysis with either 5 μ g/ml anti-Scap IgG-4H4 or 1 μ g/ml anti-Myc IgG-9E10. Films were exposed for 3-5 sec.

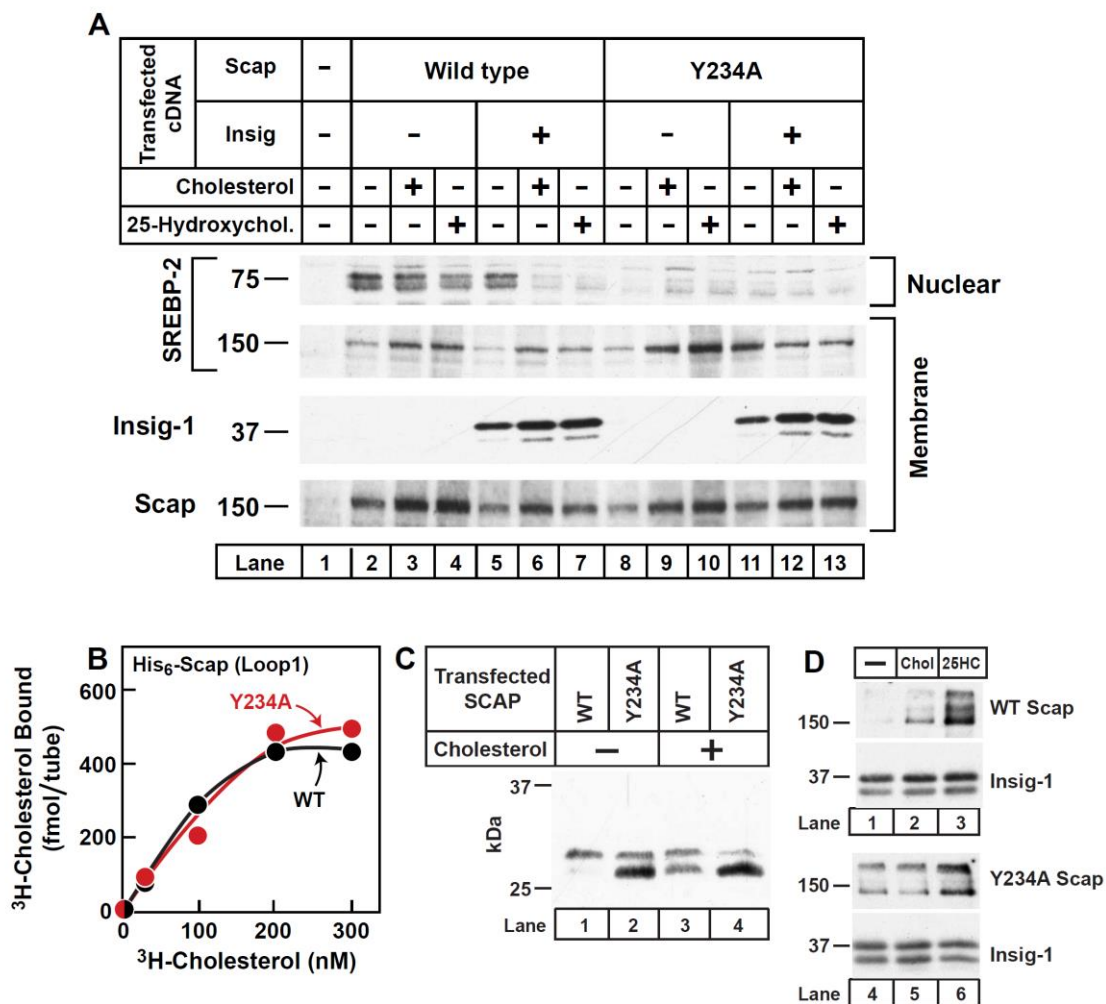
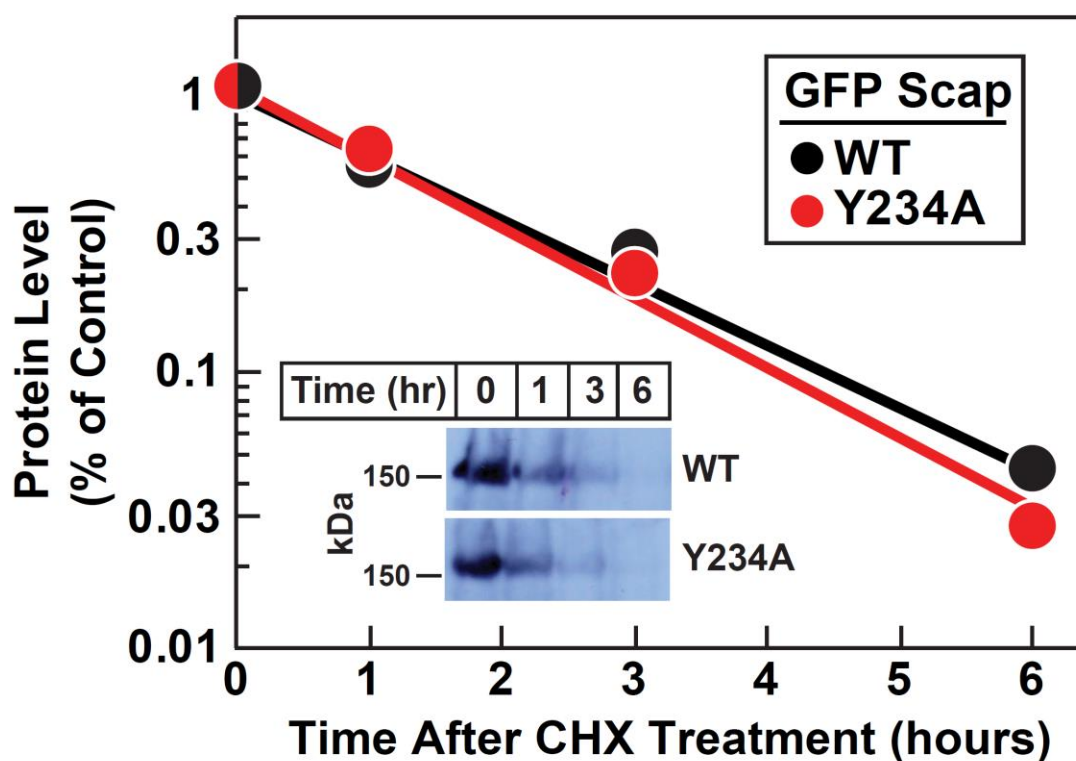
Figure 2-8

FIGURE 2-9. Cycloheximide-mediated decline in transfected WT and Y234A mutant version of GFP-Scap in CHO cells.

On day 0, CHO-K1 cells were set up for experiments in 10 ml of medium A containing 5% FCS at a density of 6×10^5 cells per 100-mm dish. On day 2, cells were transfected with 1 μ g of WT GFP-Scap or its Y239A mutant version in 7 ml of medium A supplemented with 5% FCS. FuGENE 6 was used as the transfection agent. On day 3, cells were switched to 7 ml of medium A supplemented with 5% FCS containing 50 μ M cycloheximide. At the indicated time after addition of cycloheximide, cells were washed once with PBS and then solubilized with buffer containing 1% (w/v) SDS, 10 mM Tris-HCl (pH 7.4), and 100 mM NaCl. The detergent solubilized lysate was subjected to immunoblot analysis with 1 μ g/ml anti-GFP. Film was exposed for 6 sec (*Inset*). The level of GFP-Scap protein was quantified by J. Image and plotted.

Figure 2-9



DISCUSSION

The studies in this chapter identify Loop 1 of Scap as a crucial component of the cholesterol-sensing mechanism in animal cells. When examined *in vitro*, this loop binds sterols with specificity that is identical to that of the whole membrane attachment domain (TM1-8). Moreover, a single point mutation in Loop 1 (Y234A) converts Loop 6 of Scap constitutively into the cholesterol-bound conformation as monitored by the protease protection assay. Consistent with this observation, Scap(Y234A) binds to Insig even in sterol-depleted cells, and it cannot transport SREBP-2 to the Golgi, even after sterol depletion. These findings are consistent with the protease protection assay and suggest that the MELADL sequence in Scap(Y234A) is unable to interact with COPII proteins. Precisely how a change in Loop 1 causes a change in Loop 6 is not known, but the current findings establish this interplay as a crucial element in the regulation of cholesterol metabolism in animal cells.

The way in which a luminal loop of Scap binds intramembrane cholesterol remains to be determined. When expressed in insect cells, this loop is bound tightly to membranes, most likely ER membranes. The protein cannot be released by chaotropic agents, and it requires detergents for extraction. Loop 1 contains three hydrophobic segments, as indicated in yellow in Fig. 2-1. None of these has the characteristics of a membrane-spanning helix as determined by hydrophobicity plots (see Fig. 1 of Nohturfft, *et al.*) (Nohturfft et al., 1998b). The evidence that Loop 1 lies in the ER lumen is based on studies of the glycosylation site at amino acid 263 in this loop (Fig. 2-1). This sequence was shown to be glycosylated when full-length Scap was produced in CHO cells (Nohturfft et al., 1998b). It seems likely that the hydrophobic segments in Loop 1 dip into the membrane, but do not cross it. Within the membrane, these segments would be in a position to bind intramembrane cholesterol.

Our alanine scanning mutagenesis failed to identify residues that are crucial for cholesterol binding, as indicated by the SRE-luciferase reporter assay (Fig. 2-6). It is possible that crucial cholesterol-binding residues could be identified by substituting amino acids other than alanine. Definitive identification of the cholesterol-binding site would be revealed if the structure of the loop could be studied by X-ray crystallography. Studies along these lines are under way.

In our [^3H]cholesterol-binding assays with recombinant Scap(Loop1), we used detergent concentrations that are at the borderline for micelle formation (0.004% NP-40 plus 0.001% Fos-choline-13). Moreover, we washed the nickel column and eluted the protein with solutions that lacked detergent. These conditions were determined empirically to produce an optimal ratio of specific to nonspecific [^3H]cholesterol binding. Under these conditions, we estimated that at saturation, 1 mole of [^3H]cholesterol bound to 4-5 moles of Scap(Loop1). Inasmuch as Scap(Loop1) behaved as a tetramer by gel filtration, the binding stoichiometry raises the possibility that one mole of tetramer binds one mole of cholesterol. In experiments not shown, we subjected cholesterol-bound Loop 1 to gel filtration, and the protein continued to behave as a tetramer. We therefore believe that cholesterol binding does not alter the tetrameric state. We have no data as to the oligomerization state of Scap in ER membranes. Such studies are currently in progress.

Inasmuch as a crucial residue is a tyrosine at position 234, we considered the possibility that the hydroxyl group must be phosphorylated or otherwise modified in order for Scap to exit the ER. This possibility was excluded when we substituted phenylalanine for tyrosine-234 in full length Scap and found that this protein reached the Golgi normally (data not shown).

We also considered the formal possibility that Scap(Y234A) was simply failing to fold properly and was retained in the ER through the unfolded protein response. Several observations argued strongly against this possibility: 1) Scap(Y234A) showed the appropriate cleavage patterns for the cholesterol-bound configuration when treated with trypsin (Fig. 2-8C); 2) Scap(Y234A) bound to Insig-1 (Fig. 2-8D); and 3) Scap(Y234A) and WT Scap had similar half-lives as revealed by the rate of decline of the proteins after protein synthesis was inhibited with cycloheximide (Fig. 2-9). If Scap(Y234A) were misfolded, it would be expected to be degraded more rapidly.

In earlier papers, we referred to the region of Scap containing transmembrane helices 2-6 as the “sterol-sensing domain” (Hua et al., 1996; Nohturfft et al., 1998a). This nomenclature was based on the observation that evolutionarily related sequences are present in other membrane proteins that are postulated to interact with or be influenced by sterols. The other proteins include HMG CoA reductase, an ER-bound enzyme whose degradation is accelerated by sterols (Gil et al., 1985; Skalnik et al., 1988); NPC1, a protein involved in the transport of cholesterol from lysosomes to the ER and to the plasma membrane (Carstea et al., 1997); and patched, which is the receptor for hedgehog, the only protein known to contain covalently-bound cholesterol (Porter et al., 1996). In view of the current data showing that the cholesterol-binding site in Scap is located in Loop 1 and previous data showing that the TM 2-6 segment of Scap is the Insig-binding domain (Yabe et al., 2002b; Yang et al., 2002), we will henceforth refer to the TM 2-6 segment as the Insig-binding domain (Fig. 2-1). We have not ruled out the possibility that the Insig-binding domain contains another sterol-binding site. We think this possibility is unlikely because our previous study of sterol binding to the entire TM 1-8 region of Scap showed evidence of only a single class of binding sites, and this class has the same properties as the

binding site in Loop 1. It is noteworthy that the corresponding TM 2-6 segment of HMG CoA reductase binds to Insig in a sterol-dependent fashion (Sever et al., 2003a). The roles of the corresponding transmembrane segment in NPC1 and patched remain to be determined. However, recent biochemical and crystallographic studies showed that the initial sterol-binding site in NPC1 is not contained in the transmembrane segment, but rather it lies in the N-terminal domain of the protein, which, like Loop 1 of Scap, projects into the lumen of the ER (Infante et al., 2008; Kwon et al., 2009). The current studies add important insights into the mechanisms by which a membrane protein monitors the levels of cholesterol in cell membranes. Further studies of Loop 1 of Scap promise to provide additional insights.

CHAPTER THREE

POINT MUTATION IN LUMINAL LOOP 7 OF SCAP BLOCKS INTERACTION WITH LOOP 1 AND ABOLISHES MOVEMENT TO GOLGI

SUMMARY

Scap is a polytopic protein of the endoplasmic reticulum (ER) that controls cholesterol homeostasis by transporting sterol regulatory element-binding proteins (SREBPs) from the ER to the Golgi complex. Scap has eight transmembrane helices (TM) joined by four small hydrophilic loops and three large loops. Two of the large loops (Loops 1 and 7) are in the ER lumen, and the other large loop (Loop 6) faces the cytosol where it binds COPII proteins that initiate transport to Golgi. Cholesterol binding to Loop 1 alters the configuration of Loop 6, precluding COPII binding and preventing Scap's exit from the ER. Here, we create a point mutation (Y640S) in luminal Loop 7 that prevents Scap movement to Golgi. Trypsin cleavage assays show that Loop 6 of Scap(Y640S) is always in the configuration that precludes COPII binding, even in the absence of cholesterol. When expressed separately by co-transfection, the NH₂-terminal portion of Scap (containing TM helices 1-6, including Loop 1) binds to the COOH-terminal portion (containing TM helices 7-8 and Loop 7) as determined by co-immunoprecipitation. This binding does not occur when Loop 7 contains the Y640S mutation. Co-immunoprecipitation is also abolished by a point mutation in Loop 1 (Y234A) that also prevents Scap movement. These data suggest that Scap Loop 1 must interact with Loop 7 in order to maintain Loop 6 in the configuration that permits COPII binding. These results help explain the operation of Scap as a sterol sensor.

Material from Chapter 3 was originally published in Journal of Biological Chemistry. Zhang Y, Motamed M, Seemann J, Brown MS, Goldstein JL. Point Mutation in Luminal Loop 7 of Scap Protein Blocks Interaction with Loop 1 and Abolishes Movement to Golgi. J Biol Chem. 2013 May 17; 288(20):14059-67.

INTRODUCTION

Scap is a polytopic membrane protein that binds and transports sterol regulatory element-binding proteins (SREBPs) from their sites of origin in the endoplasmic reticulum (ER) to their sites of proteolytic processing in the Golgi complex (Brown and Goldstein, 1997). After their release in the Golgi complex, the active segments of SREBPs translocate to the nucleus, where they activate all of the genes necessary to produce cholesterol and unsaturated fatty acids (Horton et al., 2002). The transport activity of Scap is mediated by the binding of COPII to a cytosolic loop (Loop 6) of Scap (Sun et al., 2005). When cholesterol levels in the ER rise above 4 – 5% of ER lipids, Loop 6 undergoes a conformational change that precludes COPII protein binding (Radhakrishnan et al., 2008; Sun et al., 2007). This change is facilitated by the binding of Scap to another ER protein called Insig (Goldstein et al., 2006). The net result is prevention of the proteolytic processing of SREBPs. As a result, cholesterol synthesis declines. This feedback mechanism ensures a constant level of cholesterol in cell membranes.

Recent studies have begun to dissect the functional domains of Scap (see Fig. 3-1). The protein has eight transmembrane helices separated by luminal and cytosolic loops (Nohturfft et al., 1998b). Three of these loops are large enough to have structure: Loops 1 and 7, which are luminal, and Loop 6, which is cytosolic. The cholesterol binding site was recently localized to luminal Loop 1 (Motamed et al., 2011). Somehow, this binding reaction in luminal Loop 1 must be communicated to cytosolic Loop 6 to change its conformation. One possibility is that luminal Loop 1 interacts with luminal Loop 7, which might alter Loop 6 through a direct action mediated by transmembrane helix 7.

We recently identified tyrosine 234 in Loop 1 as an essential residue for the transport activity of Scap. When this tyrosine is replaced by alanine (Y234A), Scap continues to bind

SREBPs, but it can no longer carry the proteins to the Golgi complex (Motamed et al., 2011). In the current studies, we have identified another crucial tyrosine at position 640 in luminal Loop 7. When this tyrosine is replaced by serine (Y640S), Scap also loses the ability to transport SREBPs. We provide evidence that these two tyrosines are necessary for the intramolecular binding between Scap segments that contain Loop 1 and those that contain Loop 7, an interaction that appears to be crucial for the transport activity of Scap.

EXPERIMENTAL PROCEDURES

Reagents—We obtained all sterols from Steraloids, Inc.; FuGENE 6 from Roche Applied Sciences; mouse anti-HSV monoclonal antibody and protease inhibitor mixture set III from Novagen; cycloheximide from Sigma; peptide-N-glycosidase F and recombinant endoglycosidaseHf from New England Biolabs; cyclodextrins from Trappsol; bovine serum albumin (catalog number 23209) from Thermo Scientific; and phRL-TK (encoding the Renilla luciferase gene) and Dual-Luciferase reporter assay system from Promega. Complexes of cholesterol with methyl- β -cyclodextrin were prepared at a stock concentration of 2.5mM (Brown et al., 2002). Newborn calf lipoprotein-deficient serum ($d > 1.215$ g/ml) was prepared by ultracentrifugation (Goldstein et al., 1983). Solutions of compactin and sodium mevalonate were prepared as described previously (Brown et al., 1978; Kita et al., 1980). A stock solution of 10mM sodium oleate-bovine serum albumin in 0.15 M NaCl (final pH 7.6) was prepared as described previously (Hannah et al., 2001). IgG-4H4, a mouse monoclonal antibody against hamster Scap (amino acids 1 – 767) (Ikeda et al., 2009), IgG-9E10, a mouse monoclonal antibody against c-Myc (Yabe et al., 2002a), and IgG-9D5, a mouse monoclonal antibody against hamster Scap (amino acids 540 – 707) (Sakai et al., 1997) were previously described in the indicated references.

Buffers—Buffer A contained 10mM Hepes-chloride (pH 7.6), 1.5 mM MgCl₂, 10mM KCl, 5 mM sodium EDTA, 5 mM sodium EGTA, and 250 mM sucrose. Buffer B contained 10 mM Tris-chloride (pH 6.8), 100 mM NaCl, and 0.5% (w/v) SDS. Buffer C contained 62.5 mM Tris-chloride (pH 6.8), 15% SDS, 8 M urea, 10% (v/v) glycerol, and 100 mM dithiothreitol. Buffer D contained 50 mM Tris-chloride (pH 7.4), 100 mM KCl, 1% (v/v) Nonidet P-40, and 1% (v/v) protease inhibitor mixture set III. Buffer E contained 50mM Tris-chloride (pH 7.4), 135mM NaCl, 10 mM KCl, 0.1% (v/v) Nonidet P-40, and 1% (v/v) protease inhibitor mixture set III.

Culture Medium—Medium A contained a 1:1 mixture of Ham' s F-12 and Dulbecco' s modified Eagle' s medium (catalog number 10-090-CV, Mediatech, Inc.) supplemented with 100 units/ml penicillin and 100 µg/ml streptomycin sulfate. Medium B contained medium A supplemented with 5% newborn calf lipoprotein-deficient serum, 50 µM sodium mevalonate, 50 µM compactin, and 1% (w/v) hydroxypropyl-β-cyclodextrin. Medium C contained medium A supplemented with 5% newborn calf lipoprotein-deficient serum, 50 µM sodium mevalonate, and 50 µM compactin. Medium D contained Dulbecco' s modified Eagle' s medium, low glucose (1000 mg/liter) supplemented with 10% fetal calf serum (FCS), 100 units/ml penicillin, and 100 µg/ml streptomycin sulfate.

Plasmids — The following recombinant expression plasmids have been previously described: pCMV-Scap, encoding hamster Scap under control of the cytomegalovirus (CMV) promoter (Sakai et al., 1997); pTK-Scap, encoding hamster Scap under control of the thymidine kinase (TK) promoter (Feramisco et al., 2005); pGFP-Scap, encoding GFP fused to hamster Scap under control of the CMV promoter (Nohturfft et al., 2000); pTK-HSV-BP2, encoding HSV-tagged human SREBP-2 under control of the TK promoter (Feramisco et al., 2005); pTK-Insig1-Myc, encoding human Insig-1 followed by six tandem copies of c-Myc epitope tag under control

of the TK promoter (Gong et al., 2006); pCMV-Insig1-Myc, encoding human Insig-1 followed by six tandem copies of a c-Myc epitope tag under control of the CMV promoter (Yabe et al., 2002b); pSRE-Luc, encoding three tandem copies of Repeat 2+Repeat 3 of the human LDL receptor promoter, the adenovirus E1b TATA box, and the firefly luciferase gene (Hua et al., 1996); pCMV-Scap(TM1 – 6)-Myc, encoding hamster Scap (amino acids 1 – 464) followed by six tandem copies of a Myc tag under control of the CMV promoter (Sun et al., 2005); and pCMV-Scap(TM7-end), encoding hamster Scap (amino acids 504 – 1276) under control of the CMV promoter (Sun et al., 2005). Point mutations in the above Scap plasmids were produced by site-directed mutagenesis. The coding regions of all mutated plasmids were sequenced.

Cell Culture and Transfection—SRD-13A cells, a Scap-deficient cell line derived from CHO-7 cells (Rawson et al., 1999), were grown in monolayer at 37 ° C in 8 – 9% CO₂ in medium A supplemented with 5% FCS, 1 mM sodium mevalonate, 20 mM sodium oleatealbumin, and 5 µg/ml cholesterol. SV589 cells, a line of SV-40 immortalized human fibroblasts (Yamamoto et al., 1984), were grown in monolayer at 37 ° C in 5% CO₂ in medium D.

Trypsin Cleavage Assay of Scap—This assay was carried out as described previously (Adams et al., 2004; Brown et al., 2002) with modifications in the culture and transfection conditions as described in the legend for Fig. 3-4B. On day 3, the cells were washed twice with PBS and switched to medium C. After incubation for 16 h at 37 ° C, the cells were harvested for preparation of membranes for use in the trypsin cleavage assay.

Co-immunoprecipitation of Scap(TM1 – 6)-Myc and Scap(TM7-end)—This assay was carried out as described previously (Motamed et al., 2011) with the use of an anti-C-Myc affinity

gel (Sigma) except for the following modification. The solubilization and wash buffers consisted of buffer D (with Nonidet P-40) supplemented with one of the following sterols: none, 1 $\mu\text{g}/\text{ml}$ 25-hydroxycholesterol (delivered in ethanol, final concentration of 0.1%), or 30 μM cholesterol complexed with methyl- β -cyclodextrin.

Assay for Scap-Insig Complex—This assay was carried out as described previously with the use of an anti-C-Myc affinity gel (Motamed et al., 2011) except for the following modifications. The pellets from two 60-mm dishes of transfected SRD-13A cells were solubilized in 0.4 ml of Nonidet P-40-containing buffer E, and the washed beads were eluted in 1x SDS sample buffer.

SREBP-2 Processing in Cultured Cells—SRD-13A cells were set up for experiments as described in the figure legends. After transfection and incubation with sterols, nuclear and membrane fractions were prepared as described previously (Feramisco et al., 2005) and then subjected to immunoblot analysis.

Immunoblot Analysis—Unless otherwise indicated, samples for immunoblotting were subjected to 8 or 10% SDS-PAGE, after which the proteins were transferred to nitrocellulose filters that were incubated at 4 ° C for 16 h with the following primary antibodies: 0.17 $\mu\text{g}/\text{ml}$ mouse monoclonal anti-HSV antibody, 1 – 5 $\mu\text{g}/\text{ml}$ mouse monoclonal anti-Myc IgG-9E10, 5 – 10 $\mu\text{g}/\text{ml}$ mouse monoclonal anti-Scap IgG-4H4, or 2.5 $\mu\text{g}/\text{ml}$ mouse monoclonal anti-Scap IgG-9D5. For all experiments except the assay for Scap-Insig complex, bound antibodies were visualized by SuperSignal West Pico chemiluminescent substrate (Thermo Scientific) using a 1:5000 dilution of anti-mouse IgG conjugated to horseradish peroxidase (Jackson ImmunoResearch Laboratories). For the experiments detecting Scap-Insig complex, bound antibodies were visualized by SuperSignal West Dura extended duration substrate using a 1:3333

dilution of anti-mouse Ig HRP (mouse TrueBlot ULTRA, eBioscience). Immunoblots were exposed to Phenix Research Products Blue x-ray film (F-BX810) at room temperature.

RESULTS

Fig. 3-1 shows a diagram of the membrane domain of Scap. The protein has eight apparent transmembrane helices and three large loops (Nohturfft et al., 1998b). Loops 1 and 7 (245 amino acids and 173 amino acids, respectively) project into the lumen of the ER. Loop 6 projects into the cytosol. Loop 6 contains the MELADL sequence that is the recognition site for COPII proteins that cluster the Scap-SREBP complex into coated vesicles for transport to the Golgi (Sun et al., 2005). When cholesterol accumulates in ER membranes, Loop 6 undergoes a conformational change that precludes COPII protein binding and abrogates ER-to-Golgi transport (Sun et al., 2007). When expressed as a recombinant protein segment, Loop 1 binds cholesterol *in vitro* (Motamed et al., 2011). The specificity of sterol binding to Loop 1 mimics the binding specificity of sterol binding to the entire membrane domain of Scap. A point mutation in Loop 1 (Y234A) renders Loop 6 of Scap in the closed COPII-inaccessible configuration even in sterol-depleted membranes and abrogates movement to the Golgi (Motamed et al., 2011). The other large intraluminal loop (Loop 7) is the subject of the current study.

In an initial attempt to characterize the function of Loop 7, we conducted an alanine-scanning mutagenesis study of the entire loop by systematic replacement of every pair or trio of contiguous residues with alanines. Plasmids encoding the mutant Scaps were transfected into Scap-deficient SRD-13A CHO cells together with a plasmid encoding firefly luciferase under control of an SRE-dependent promoter. To control for transfection efficiency, we also transfected a plasmid encoding Renilla luciferase driven by a constitutive thymidine kinase

promoter, and we included a plasmid encoding Insig-1 to assist in the sterol-mediated inhibition of Scap transport. As shown in Fig. 3-2A, most of the Loop 7 mutants behaved like wild-type Scap in restoring SREBP cleavage as measured by the sterol-regulated increase in luciferase activity. Four of the mutants showed a marked reduction in the ability to elicit activation of the SRE dependent promoter (indicated by red asterisks). All of these defective mutants clustered in the region of Scap between residues 640 and 657.

All four of the severely defective mutants in Fig. 3-2A consisted of three contiguous alanine substitutions. When any of the individual residues in these triplets were changed to alanine, there were only minor losses of function (Fig. 3-2B). Reasoning that the single alanine substitutions were not drastic enough to perturb function, we selected three hydrophobic residues (Tyr-640, Tyr-648, and Ile-655) and replaced them individually with hydrophilic or charged residues (Ser, Gln, Asp, or Lys). Several of these single substitutions severely reduced SREBP-dependent luciferase activity (Fig. 3-2C). For further study, we chose Y640S.

To study SREBP cleavage directly, we transfected plasmids encoding WT or Y640S Scap into Scap-deficient SRD-13A cells together with a plasmid containing epitope-tagged SREBP-2. Expression of Scap was driven by the weak TK promoter so as to produce low level expression of Scap, which does not overwhelm endogenous Insigs and thereby facilitates sterol-dependent inhibition of processing. Cells were incubated in sterol depleted medium with or without added cholesterol. After cells were harvested, nuclear extracts and membrane fractions were prepared and subjected to SDS-PAGE and immunoblotting. As reported previously (Yang et al., 2002), in the absence of Scap, we failed to visualize a nuclear fragment of SREBP-2 (Fig. 3-3A, lane 1). SREBP-2 was also not observed in the membrane fraction because the membrane-bound precursor is rapidly degraded in the absence of Scap (Rawson et al., 1999). When WT Scap was

co-transfected, we visualized the membrane form of SREBP-2, indicating that the precursor was stabilized (lanes 2 and 3). We also observed the nuclear form of SREBP-2, and this was reduced by cholesterol. The Y640S Scap mutant stabilized the membrane precursor form of SREBP-2, indicating that it bound the precursor, but it did not generate any nuclear form (lanes 4 and 5). When Insig-1 was transfected together with WT Scap, we observed a more profound cholesterol-mediated reduction in nuclear SREBP-2 (lanes 6 and 7). Again, Scap Y640S stabilized the membrane form of SREBP-2, but it did not generate the nuclear form (lanes 8 and 9). We blotted the membrane fractions with antibodies to the epitope tags on Scap and Insig-1 to show that comparable levels were expressed in all of the transfected cells.

We previously showed that overexpression of WT Scap, driven by the strong CMV promoter, saturates Insig and prevents cholesterol from blocking the transport and cleavage of SREBP-2 (Yang et al., 2000). To test whether the Y640S mutant would also saturate Insig, we transfected a plasmid encoding Scap(Y640S) driven by the CMV promoter. As shown in Fig. 3-3B, transfection of TK-driven WT Scap stabilized the membrane SREBP-2 precursor and restored cleavage in the SRD-13A cells, and cleavage was reduced by cholesterol (lanes 1 – 3). Scap(Y640S) stabilized the SREBP-2 precursor, but it did not restore cleavage even when driven by the strong CMV promoter (lanes 4 and 5). Importantly, when co-transfected together with WT Scap, the CMV-driven Scap(Y640S) prevented cholesterol-mediated suppression of SREBP-2 cleavage (lanes 6 and 7). This prevention persisted even when we co-transfected a plasmid encoding Insig-1 (lanes 12 and 13). These data indicate that Scap(Y640S) is capable of binding and saturating Insig-1, a conclusion that was confirmed by direct co-immunoprecipitation (see below).

We previously showed that WT Scap becomes glycosylated in the ER, and the carbohydrates are sensitive to removal by endoglycosidase H (Nohturfft et al., 1998a). Fig. 3-4A repeats this result and shows that the Y640S mutant is similarly glycosylated. In Fig. 3-4B, we used our previously described trypsin digestion assay (Adams et al., 2004; Brown et al., 2002) to detect the cholesterol-induced change in the conformation of Loop 6 of WT Scap and the Y640S and Y234A mutants. SRD-13A cells were transfected with plasmids encoding one of these proteins. Sealed membrane vesicles were prepared, incubated with varying amounts of cholesterol, and digested with trypsin followed by treatment with peptide-N-glycosidase F and SDS-PAGE. A trypsin-protected fragment of Scap was visualized by blotting with a monoclonal antibody directed against luminal Loop 7 (Fig. 3-1). In the absence of cholesterol, WT Scap gave a single band of 250 amino acids at ~30 kDa (lane 2), which is produced by trypsin cleavage at arginine 496 and a cluster of arginines at residues 747 – 750 (Brown et al., 2002) (Fig. 3-1). In the presence of cholesterol, a new trypsin-protected band of ~241 amino acids was detected (lanes 5 and 8). The lower band is generated by cleavage at arginines 503/505, which become exposed to trypsin as a result of a cholesterol-induced conformation change in Scap Loop 6 (Adams et al., 2004; Brown et al., 2002). The Y640S and Y234A mutants both showed the lower band even in the absence of cholesterol (lanes 3 and 4). When cholesterol was added to the Y640S mutant, the upper band disappeared and the lower band increased (lanes 6 and 9). In contrast, the Y234A mutant showed little change in the presence of cholesterol (lanes 7 and 10).

To confirm the interaction of Scap(Y640S) with Insig-1, we performed a co-immunoprecipitation experiment (Fig. 3-4C). SRD-13A cells were transfected with plasmids encoding Myc- tagged Insig-1 and WT or Y640S Scap. The cells were incubated in the absence of sterols or in the presence of cholesterol or 25-hydroxycholesterol. Membranes were

solubilized, and the Myc-tagged Insig-1 was precipitated on anti-Myc beads. The eluted proteins were blotted with anti-Scap or anti-Insig-1. In the absence of Insig-1 expression, no WT Scap was precipitated by the anti-Myc beads (lane 1). When Myc-Insig-1 was expressed, a small amount of Scap was co-immunoprecipitated (lane 2), and this increased when cholesterol or 25-hydroxycholesterol was added to the cells (lanes 3 and 4). In the absence of sterols, Scap(Y640S) was co-precipitated with Myc-Insig-1 (lane 5), and there was no further increase when cholesterol or 25-hydroxycholesterol was added (lanes 6 and 7). These data indicate that Scap(Y640S) retains the ability to bind to Insig-1, and it does so even in the absence of cholesterol.

The failure of Scap(Y640S) to reach the Golgi was confirmed by the immunofluorescence experiment of Fig. 3-5. SV589 cells were transfected with a plasmid encoding GFP-tagged WT Scap or the Y640S mutant. The cells were incubated with hydroxypropyl- β -cyclodextrin to remove cholesterol and stimulate Scap translocation to the Golgi. We included cycloheximide to minimize fluorescence due to newly synthesized Scap. The cells were permeabilized and immunostained for the Golgi marker GM130 using an antibody conjugated to Alexa Fluor 594, which fluoresces red. We also added Hoechst 33342, which stains nuclei blue. With WT Scap, the GFP signal was concentrated in discrete particles that stained for GM130, indicating that they represented Golgi stacks (upper panels). In sharp contrast, the GFP-tagged Scap(Y640S) showed a lacy distribution consistent with retention in the ER (lower panels). The images shown in Fig. 3-5 are representative of many transfected cells that were examined individually. Of the 1565 transfected WT cells examined, Scap was localized to the ER in 15% of cells and to the Golgi in 85% of cells, whereas in the 1000 transfected Y640S mutant cells examined, Scap was visualized in the ER in >98% of cells.

Previously, we transfected cells simultaneously with a plasmid encoding the TM1 – 6 portion of Scap and a second plasmid encoding the remainder of the protein (TM7 to the COOH terminal end of the WD repeat domain)(Sun et al., 2007; Yang et al., 2000). We refer to the latter portion as TM7-end (Fig. 3-6A). We showed that these two segments interact with each other as measured by co-immunoprecipitation assays and that they reconstitute SREBP transport activity. Fig. 3-6B shows a co-immunoprecipitation experiment in which we transfected SRD-13A cells with a plasmid encoding either WT or the Y234A mutant version of Myc-tagged TM1 – 6 together with a second plasmid encoding WT TM7-end. We also transfected the cells with WT TM1 – 6 together with Y640S(TM7-end). Cells were incubated in the absence of sterols or in the presence of cholesterol or 25-hydroxycholesterol. We isolated the Myc-tagged TM1 – 6 segment on anti-Myc beads, eluted the bound proteins, and probed immunoblots with an antibody against TM7-end. When both segments were WT, the TM7-end was co-immunoprecipitated with TM1 – 6 (see pellet in bottom panel, lane 3). There was little effect when the cells were incubated with 25-hydroxycholesterol (lane 5). In contrast, cholesterol reduced the amount of co-immunoprecipitated Scap(TM7-end) by about 50%. We observed a similar 50% reduction in more than 10 experiments in which we varied the ratio between the TM1 – 6 fragment and the TM7-end fragment and in which we performed the co-immunoprecipitation with or without cotransfection with a plasmid encoding Insig-1. All of these experiments were performed by exposing the cells to maximal concentrations of cholesterol/methyl- β -cyclodextrin (30 μ M). In none of the experiments did 25-hydroxycholesterol reduce the co-immunoprecipitation. As shown in Fig. 3-6B, lanes 6 – 8, the Y640S mutant TM7-end segment failed to co-immunoprecipitate with the WT TM1 – 6 segment. Similarly, the Y234A mutant TM1 – 6 failed

to co-immunoprecipitate with WT TM7-end (lanes 9 – 11). Thus, point mutations either in Loop 1 or in Loop 7 can abolish the interaction between the TM1 – 6 segment and the TM7-end segment of Scap.

FIGURE 3-1. Topology model of the membrane domain of hamster Scap, showing its three functional domains and the sites of three point mutations (Y234A, D428A, and Y640S) that confer a constitutive cholesterol-bound conformation, even in the absence of sterols.

Amino acids (aa) 40–284 correspond to the sequence of luminal Loop 1, the cholesterol-binding domain of Scap. The three hydrophobic patches in the Loop 1 sequence are shaded in purple, and the N-linked glycosylation site is denoted by the red box. The Insig-binding domain is localized to transmembrane helices 2–6, shown by the blue bracket. The COPII-binding site is localized to the MELADL sequence in Loop 6, shaded in orange. Amino acids 538–710 correspond to the sequence of luminal Loop 7; its two N-linked glycosylation sites are denoted by the red boxes. In membranes from sterol-deprived cells, trypsin cleaves Scap on its NH₂-terminal side at Arg-496; in sterol-replete membranes, trypsin cleaves at Arg-503/Arg-505. The trypsin-cleavage site on the COOH-terminal side of Scap in both the absence and the presence of sterols occurs within a cluster of arginines (Arg-747–Arg-750).

Figure 3-1

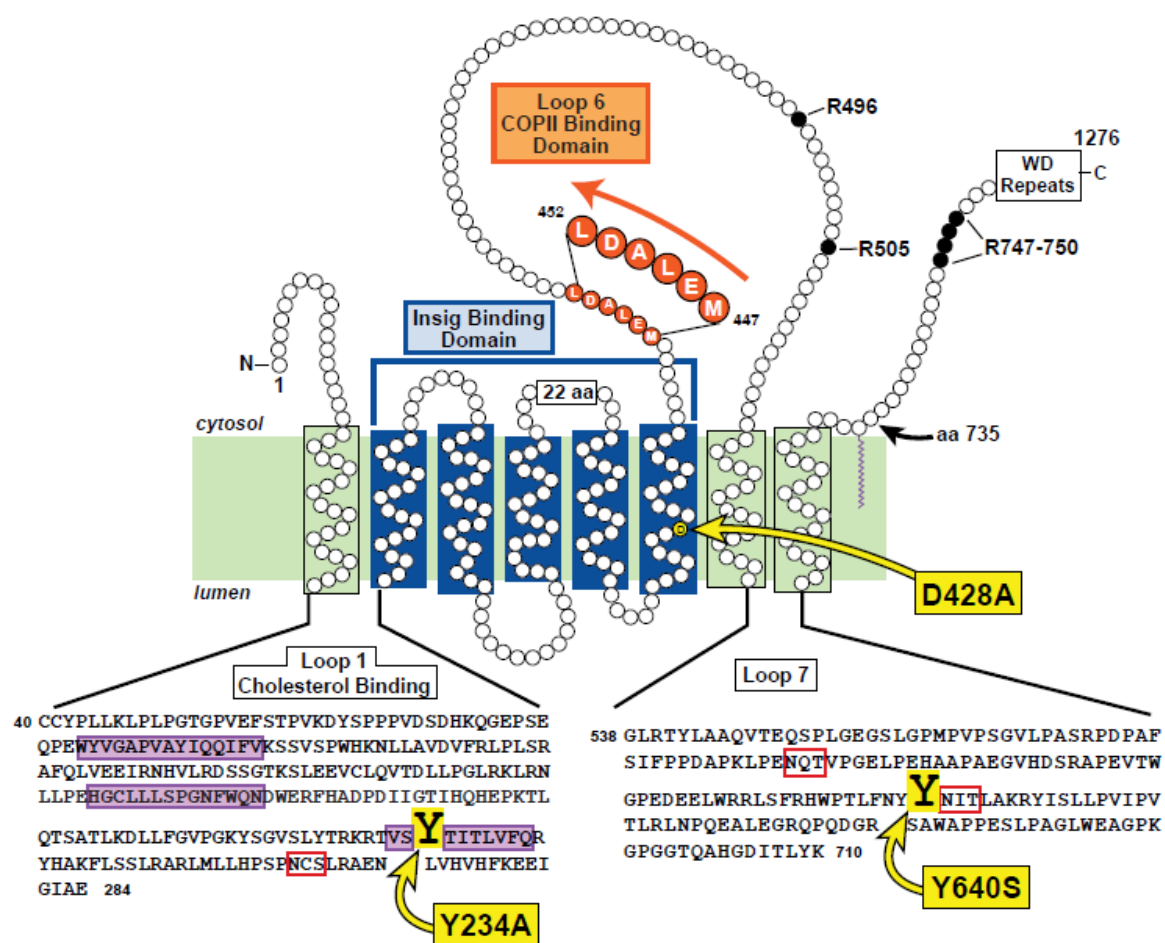


FIGURE 3-2. Alanine-scanning mutagenesis of Loop 7 region of hamster Scap.

On day 0, SRD-13A cells were set up for experiments in 1 ml of medium A containing 5% FCS at a density of 2.5×10^4 cells/well in 24-well plates. On day 1, cells were co-transfected in 1 ml of medium A supplemented with 5% FCS containing 38 ng of pTK-Insig1-Myc, 125 ng of pSRE-firefly luciferase, 125 ng of pTK-Renilla luciferase, and 50 ng of WT or the indicated mutant pTK-Scap in which 2–3 contiguous residues were mutated to alanine. FuGENE 6 was used as the transfection agent. For each transfection, the total amount of DNA was adjusted to 338 ng/dish by the addition of pcDNA mock vector. On day 2 (after incubation with plasmids for 24 h), the cells were washed once with PBS and then treated with hydroxypropyl- β -cyclodextrin-containing medium B for 1 h. Cells were then washed twice with PBS and re-fed with 1 ml of medium C in the absence or presence of 15 μ M cholesterol complexed with methyl- β -cyclodextrin. After incubation for 16 h, the cells were washed with PBS, after which luciferase activity was read on a Synergy 4 plate reader (BioTek) according to the Promega protocol. The amount of SRE-firefly luciferase activity in each dish was normalized to the amount of Renilla luciferase activity in the same dish. Relative SRE-luciferase activity of 1.0 represents the normalized luciferase value in dishes transfected with WT pTK-Scap in the absence of cholesterol. All values are the average of duplicate assays. A, red asterisks denote triple contiguous alanine mutations that produced a loss of SRE-luciferase activity in both the absence and the presence of cholesterol. The data in these graphs were obtained in four different experiments, each with its own WT control. B, deconvolution of triple mutants that showed loss of SRE-luciferase activity in A. Blue boxes denote single alanine mutations that show partial loss of SRE-luciferase activity. C, substituting serine, glutamine, aspartic acid, and lysine in place of

Tyr-640, Tyr-648, and Ile-655. The red arrow denotes the Y640S mutation that was selected for further characterization. In B and C, single-letter codes are used to denote amino acids.

Figure 3-2

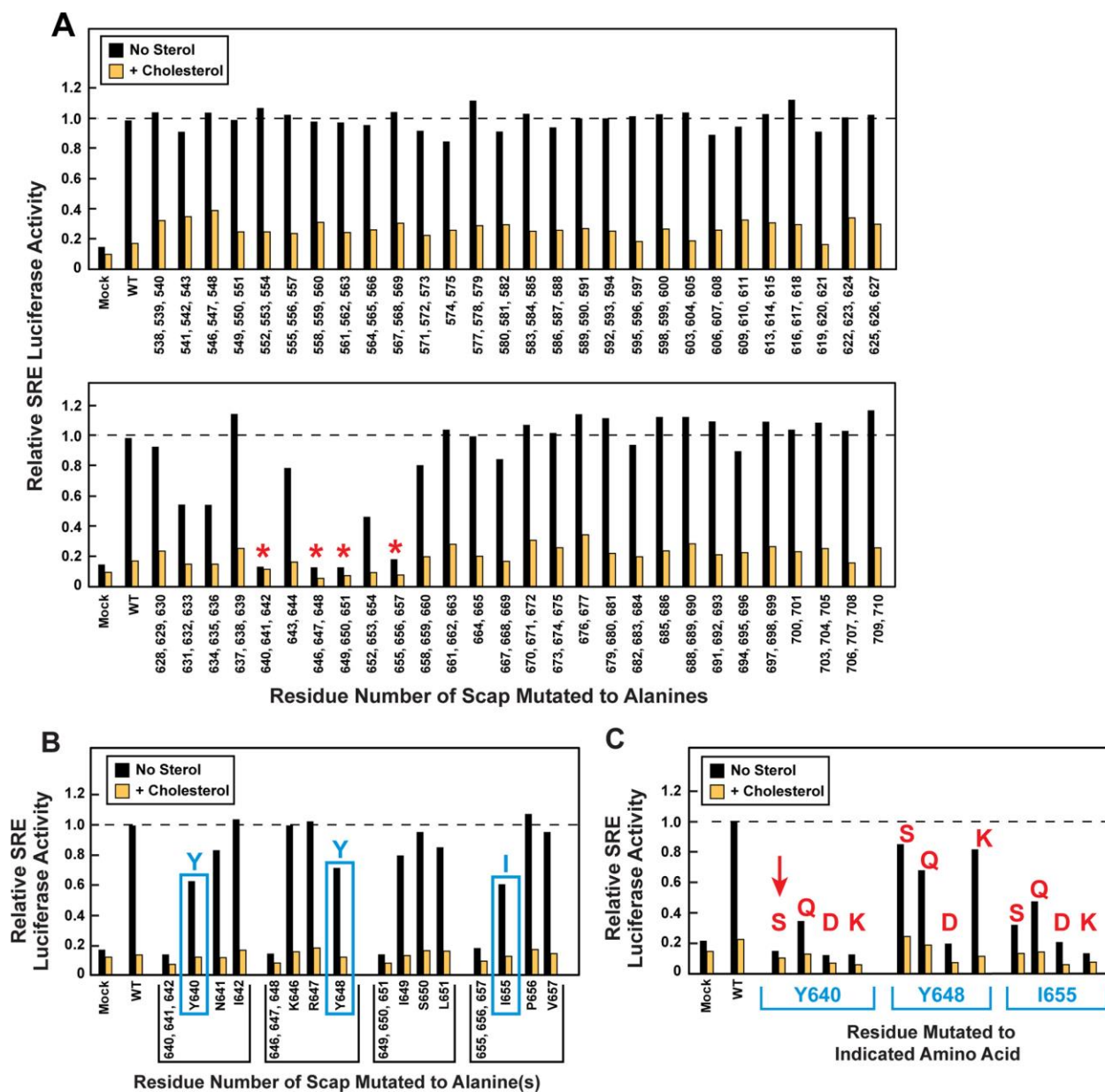


FIGURE 3-3. Immunoblot analysis of SREBP-2 cleavage in Scap-deficient cells transfected with WT or Y640S mutant version of full-length Scap in the absence or presence of transfected Insig-1.

A, Y640S mutant driven by TK promoter. On day 0, SRD-13A cells were set up for experiments at a density of 2.5×10^5 cells/60-mm dish in 4ml of medium A containing 5% FCS. On day 2, cells were transfected with 2 μ g of pTK-HSV-BP2 and 0.4 μ g of full-length WT pTK-Scap or 0.6 μ g of its Y640S version with or without 0.2 μ g of pTKInsig1-Myc in 3 ml of medium A supplemented with 5% FCS; FuGENE 6 was used as the transfection agent. For each transfection, the total amount of DNA was adjusted to 2.8 μ g/dish by the addition of pcDNA mock vector. On day 3, cells were washed once with PBS and then switched to hydroxypropyl- β -cyclodextrin-containing medium B for 1 h. The cells were washed with PBS and then incubated with medium C containing 30 μ M cholesterol complexed with methyl- β -cyclodextrin as indicated. After incubation for 4 h, two pooled dishes of cells per condition were harvested, and the isolated nuclear and membrane fractions were subjected to immunoblot analysis with 0.167 μ g/ml anti-HSV (SREBP-2), 1 μ g/ml anti-Myc IgG-9E10 (Insig-1), or 5 μ g/ml IgG-4H4 (Scap). B, Y640S mutant driven by CMV promoter. Experimental design was as in A except for DNA transfections. Cells were transfected with 2 μ g of pTK-HSV-BP2 together with one of the following additional plasmids: none (lane 1); 0.4 μ g of full-length WT pTK-Scap (lanes 2, 3, 8, and 9); 0.6 μ g of mutant pCMV-Scap(Y640S) (lanes 4, 5, 10, and 11); or 0.4 μ g of WT pTK-Scap plus 0.6 μ g of mutant pCMV-Scap(Y640S) (lanes 6, 7, 12, and 13) with or without 0.2 μ g of pTK-Insig1-Myc as indicated. For each transfection, the total amount of DNA was adjusted to 3.2 μ g/dish by the addition of pcDNA mock vector. Films were exposed for 1–20 s.

Figure 3-3

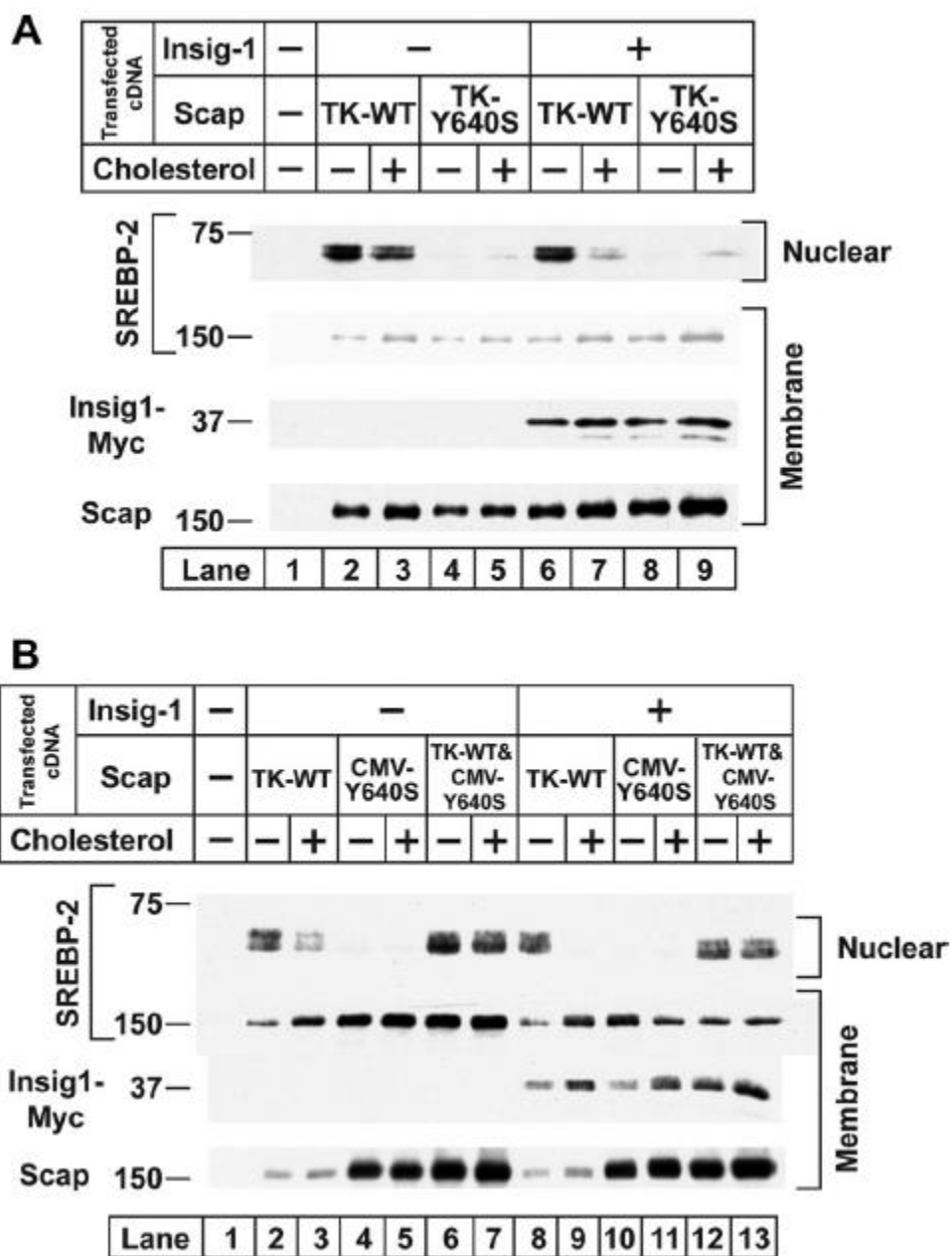


FIGURE 3-4. Biochemical characterization of Y640S Scap.

A–C, on day 0, Scap deficient SRD-13A cells were set up for experiments at a density of 2.5×10^5 cells/60-mm dish in 4ml of medium A containing 5% FCS. On day 2, cells were transfected with the indicated plasmid using FuGENE 6 as the transfection agent. A, endoglycosidase H (Endo H) sensitivity. Transfected cDNAs were as follows: 2 μ g of pcDNA mock vector (lanes 1 and 2), WT pTK-Scap (lanes 3 and 4), or mutant pTK-Scap(Y640S) (lanes 5 and 6) in 3 ml of medium A supplemented with 5% FCS. On day 3, five pooled dishes of cells were harvested per condition, washed with PBS, lysed in 1ml buffer A containing protease inhibitors (Wang et al., 2010) by passing through a 22-gauge needle 30 times. The lysate was centrifuged at 1000xg for 5 min at 4 °C, after which the supernatant was centrifuged at 20,000xg for 30 min at 4 °C. The pellet was then resuspended in 100 μ l buffer B and shaken for 30 min at room temperature. Reactions, in a final volume of 100 μ l buffer B, contained 40 μ g of solubilized membranes and 0.16 mM dithiothreitol in the absence or presence of 5000 units of endoglycosidase H. After incubation at 37 °C for 3 h, an equal volume of buffer C was added to each reaction and incubated at 37 °C for 30 min. Samples were then subjected to 8% SDS-PAGE and immunoblotted with 5 μ g/ml IgG-4H4 (Scap). The film was exposed for 15 s. B, tryptic digestion. On day 2, SRD-13A cells were transfected with 1 μ g of the indicated full-length WT or mutant version of pCMV-Scap plasmid. After incubation with lipoprotein-deficient serum for 16 h, three dishes of cells were harvested per condition and pooled for preparation of membranes. Aliquots of the 20,000xg membrane fraction (100 μ g) were incubated for 20 min at room temperature with the indicated concentration of cholesterol complexed with methyl- β -cyclodextrin (Chol.) followed by sequential treatments with 14 μ g/ml trypsin (30 min at 30 °C) and 3000 units/ml peptide-N-glycosidase F (5 h at 37 °C). By removing N-linked sugars,

peptide-N-glycosidase F increases the separation between the upper and lower trypsin-generated bands. The air-dried acetone-precipitated samples were then subjected to SDS-PAGE and immunoblot analysis with 5 $\mu\text{g/ml}$ anti-Scap IgG-4H4. The film was exposed for 5 s. C, immune detection of Scap-Insig-1 complexes. On day 2, cells were co-transfected with 0.1 μg of pCMV-Insig1-Myc together with 0.3 μg of full-length WT pCMV-SCAP or its mutant Y640S version as indicated. On day 3, the cells were incubated for 1 h with 1% (w/v) hydroxypropyl- β -cyclodextrin, after which they received fresh medium containing one of the following sterols: none (-), 50 μM cholesterol complexed with methyl- β -cyclodextrin (Chol), or 1 $\mu\text{g/ml}$ 25-hydroxycholesterol (25HC). After incubation at 37 $^{\circ}\text{C}$ for 4 h, the cells were harvested and lysed. Lysates from two pooled dishes were incubated with anti-Myc beads to trap Insig-1. After washing, the proteins were eluted by incubation for 5 min at 37 $^{\circ}\text{C}$ with 1x SDS sample buffer. The eluates were subjected to immunoblot analysis with either 10 $\mu\text{g/ml}$ anti-IgG-4H4 (Scap) or 5 $\mu\text{g/ml}$ anti-Myc IgG-9E10 (Insig-1 Myc). Films were exposed for 4–30 s.

Figure 3-4

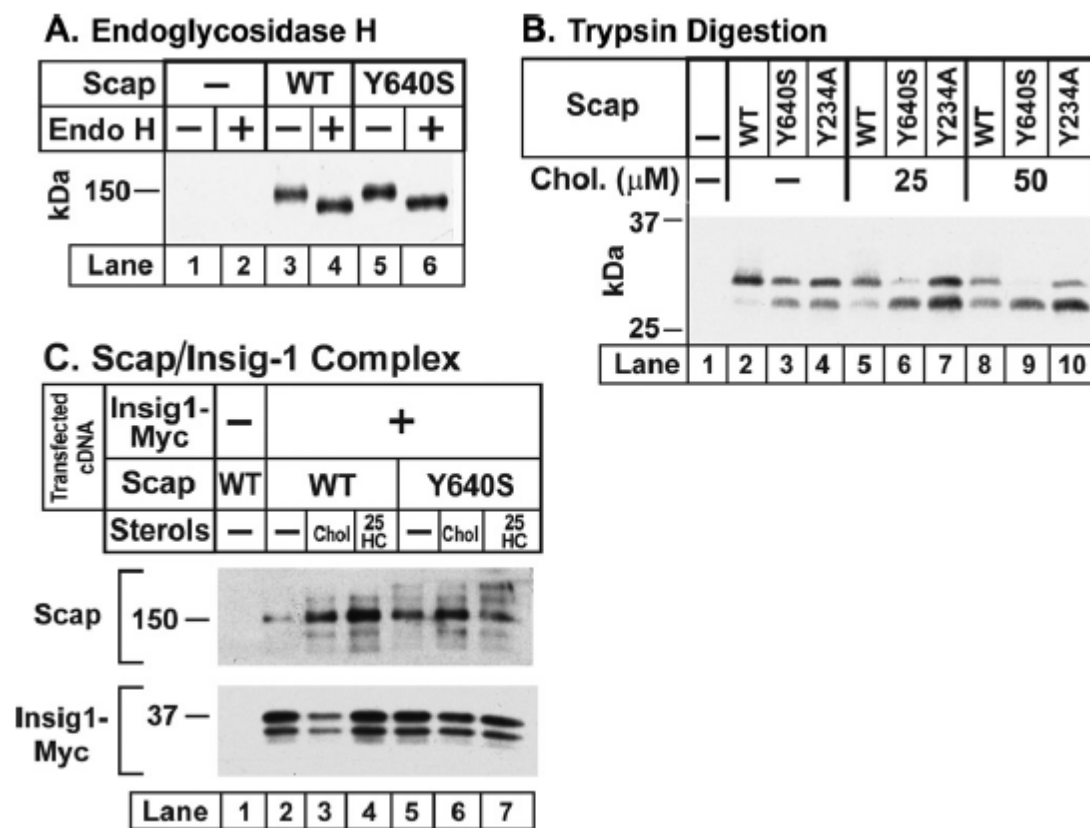


FIGURE 3-5. Mutant GFP-Scap (Y640S), but not WT GFP-Scap, fails to reach the Golgi.

On day 0, SV589 cells (Yamamoto et al., 1984) were set up for experiments in medium D at a density of 1×10^5 cells/37-mm dish containing three 12-mm glass coverslips. On day 1, cells were transfected with 1 μ g of full-length WT pGFP-Scap (top panels) or its mutant Y640S version (bottom panels) in 3 ml of medium A supplemented with 5% FCS. FuGENE 6 was used as the transfection reagent. On day 2, the cells were washed once with PBS and then incubated for 1 h at 37 °C with cyclodextrin-containing medium B supplemented with 50 μ g/ml cycloheximide, after which each coverslip was fixed and permeabilized in methanol at -20 °C for 15 min. The cells were then incubated with rabbit polyclonal serum against the Golgi resident protein GM130 (Wei and Seemann, 2009b) followed by 6.7 μ g/ml goat anti-rabbit antibody conjugated to Alexa Fluor 594 (Invitrogen). The nuclei were then stained with 1 μ g/ml Hoechst 33342 (Invitrogen), and the coverslips were mounted in Mowiol 4-88 (Calbiochem) mounting solution (Wei and Seemann, 2009a). Fluorescence images were acquired using an LD Plan-Neofluar 40x/1.3 differential interference contrast objective, an Axiovert 200M microscope (Zeiss), an Orca 285 camera (Hamamatsu), and the software Openlab 4.0.2 (Improvision). Scale bar, 10 μ m.

Figure 3-5

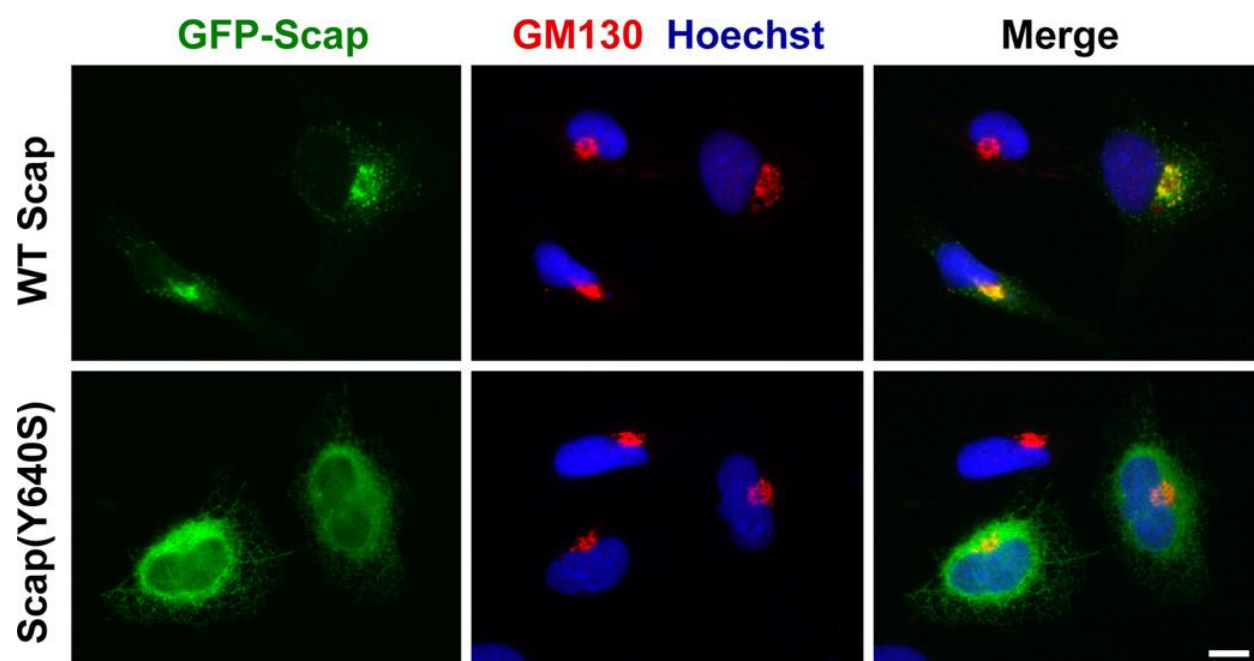
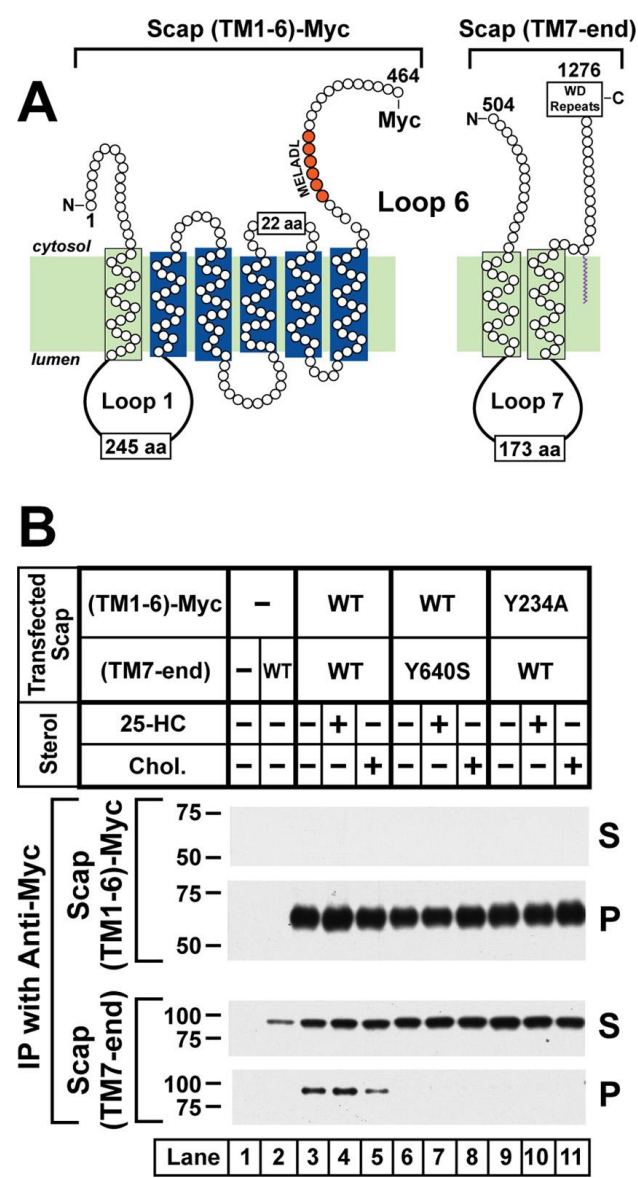


FIGURE 3-6. Co-immunoprecipitation of NH₂- and COOH-terminal segments of WT Scap, but not mutant Scap(Y640S).

A, membrane topology of hamster Scap denoting NH₂- and COOH-terminal segments encoded by two different cDNAs. Scap(TM1–6)-Myc encodes hamster Scap (amino acids (aa) 1–464) followed by six tandem copies of a Myc tag under control of the CMV promoter (Sun et al., 2005). Scap(TM7-end) encodes hamster Scap (amino acids 504–1276) under control of the CMV promoter (Sun et al., 2005). B, co-immunoprecipitation (IP). On day 0, Scap-deficient SRD-13A cells were set up for experiments in 3 ml of medium A containing 5% FCS at a density of 2.5×10^5 cells/60-mm dish. On day 2, cells were transfected in 3ml of medium A containing 5% FCS with the following plasmids: 2.5 μ g of pTK-HSV-BP2 (lanes 1–11); 2 μ g of pCMVSCAP(TM1–6)-Myc (lanes 3–8); 2 μ g of the mutant Y234A version of pCMVSCAP(TM1–6)-Myc (lanes 9–11); 0.5 μ g of pCMV-SCAP(TM7-end) (lanes 2–5 and 9–11); and 0.5 μ g of the mutant Y640S version of pCMV-SCAP(TM7-end) (lanes 6–8). FuGENE 6 was used as the transfection agent. The total amount of DNA was adjusted to 5 μ g/dish by the addition of pcDNA mock vector. 12 h after transfection, the cells were incubated in medium C in the absence (lanes 1–3, 6, and 9) or presence of either 1 μ g/ml 25-hydroxycholesterol (25-HC) (delivered in ethanol, final concentration of 0.1%) (lanes 4, 7, and 10) or 30 μ M cholesterol complexed with methyl- β -cyclodextrin (Chol.) (lanes 5, 8, and 11). After incubation for 12 h, each detergent-solubilized whole cell lysate from two pooled dishes was incubated with anti-Myc beads followed by washing and elution with Myc peptide as described under “Experimental Procedures.” The eluates were subjected to immunoblot analysis with either 1 μ g/ml anti-Myc IgG-9E10 (Scap(TM1–6)-Myc) or 2.5 μ g/ml anti-IgG-9D5 (Scap(TM7-end)). The film was exposed for 1–10 s. S, supernatant; P, pellet.

FIGURE 3-6



DISCUSSION

In a previous study, we showed that cholesterol binds to luminal Loop 1 of Scap. We also created a point mutation in Loop 1 (Y234A) that rendered Scap unable to transport SREBP-2 to the Golgi complex even in the absence of sterols (Motamed et al., 2011). We used trypsin digestion assays to assess the conformation of Loop 6, which contains the MELADL sequence that binds COPII proteins. These digestions revealed that Loop 6 was in the closed conformation (i.e. the conformation that does not bind COPII proteins) even in the absence of sterols. In the current studies, we have created a point mutation in the other large luminal domain of Scap (Loop 7) that has the same effects as the Loop 1 mutation. In cells expressing Scap with this Y640S mutation, Loop 6 also assumed the closed conformation in the absence of sterols (Fig. 3-4B). Scap(Y640S) also failed to transport SREBPs to the Golgi as revealed by SREBP processing assays (Fig. 3-3A) and by immunofluorescence localization (Fig. 3-5).

We considered the possibility that Scap(Y640S) is misfolded and therefore precluded from exiting the ER through the action of the ER quality control system. Several observations argue against this possibility. First, Scap(Y640S) stabilizes the membrane precursor of SREBP-2, which is rapidly degraded in the absence of Scap (Fig. 3-3A) (Rawson et al., 1999). Second, Scap(Y640S) binds Insig-1 as determined by direct co-immunoprecipitation (Fig. 3-4C) and by the observation that overexpression of Scap(Y640S) saturated Insig-1 and allowed WT Scap to carry SREBPs to the Golgi even in the presence of cholesterol (Fig. 3-3B). We conclude that Scap(Y640S) is properly folded.

The fact that point mutations in Loop 1 and Loop 7 block Scap movement raises the possibility that these two loops must interact in order for this movement to occur. This hypothesis is supported by the co-immunoprecipitation experiment of Fig. 3-6. When we

expressed WT Scap(TM1 – 6) and WT Scap(TM7- end) in the same cells, the two proteins bound to each other, and they could be co-immunoprecipitated. When either the mutant TM1 – 6 segment or the mutant TM7-end segment was substituted for the corresponding WT segment, co-immunoprecipitation was abolished. Cholesterol reduced the amount of co-immunoprecipitation by about 50% (Fig. 3-6B, lane 5). This result was reproduced in more than 10 other experiments. In all of these experiments, 25-hydroxycholesterol failed to reduce the co-immunoprecipitation. This failure persisted even when we co-expressed Insig-1 by transfection.

Interaction of luminal Loop 1 of Scap with luminal Loop 7 provides a potential mechanism by which binding of cholesterol to Loop 1 would alter the conformation of cytosolic Loop 6. If cholesterol binding changes the conformation of Loop 1, and if this is transmitted to Loop 7, then Loop 7 might alter the conformation of Loop 6 through some effect on transmembrane helix 7, which joins the two loops (Fig. 3-1). The interaction between Loops 1 and 7 might occur within a single Scap monomer or between adjacent molecules in the Scap tetramer (Radhakrishnan et al., 2004). The failure of 25-hydroxycholesterol to reduce the co-immunoprecipitation between Scap(TM1 – 6) and Scap(TM7-end) might be explained by our previous observation that 25-hydroxycholesterol blocks Scap movement not by binding to Scap, but rather by binding to Insig (Radhakrishnan et al., 2007; Sun et al., 2007). Our findings therefore raise the possibility that the 25-hydroxycholesterol-Insig complex directly blocks COPII binding to the MELADL sequence in Scap Loop 6 without a requirement for dissociation between Loop 1 and Loop 7. Experiments are under way to test these hypotheses.

CHAPTER FOUR

CONCLUSION AND PERSPECTIVE

This thesis has focused on understanding the biochemical basis for sterol sensing in Scap, the protein that controls cholesterol homeostasis in animal cells. We highlight the importance of two luminal loops unique in Scap whose functions were not appreciated previously. One large luminal loop, Loop 1, is directly involved in sterol recognition; another large luminal loop, Loop 7, must interact with Loop 1 to transduce the sterol-binding signal to control Scap movement. These studies indicate that cholesterol recognition and response is not deep in the membrane as previously thought, but somehow in its periphery.

When examined *in vitro*, Scap Loop 1 binds cholesterol with 50-100nM affinity and a sterol specificity that is identical to that of the whole membrane attachment domain (TM1-8). It should be noted that Scap Loop 1 is bound tightly to membranes and is insoluble without detergents. And cholesterol has extremely low solubility in water (Gilbert et al., 1975). Developing an assay to study a hydrophobic polypeptide binding to a hydrophobic ligand in aqueous solution was difficult and very tricky. We had to determine conditions empirically to produce an optimal ratio of specific to nonspecific [³H] cholesterol binding.

We have not yet identified a cholesterol-binding mutation in Loop 1 through alanine-scanning mutagenesis using the SRE-luciferase reporter assay. It is possible that crucial cholesterol-binding residues could be found by substituting amino acids other than alanine. X-ray crystallography is needed to definitively identify the cholesterol-binding pocket and also guide the cholesterol-binding mutation design.

We have not ruled out the possibility that Scap contains another sterol-binding site besides Loop 1. We think this possibility is unlikely because our previous study of sterol binding to the entire TM 1-8 region of Scap showed evidence of only a single class of binding sites, and this class has the same properties as the binding site in Loop 1. Thus, the evolutionarily conserved TM2-6 in Scap, so called “sterol-sensing domain”, is unlikely to be involved in direct sterol binding, but rather functions as an effector domain. Indeed, previous data show that TM2-6 in Scap and an evolutionarily related TM2-6 in HMG CoA reductase both bind to Insig in a sterol-dependent fashion (Sever et al., 2003b; Yabe et al., 2002b; Yang et al., 2002). Thus, the “sterol-sensing domain” is in fact an Insig-binding domain.

If cholesterol first binds to luminal Loop 1, the signal must be transmitted across the membrane to cytosolic Loop 6, which interacts with COPII proteins that initiate movement to the Golgi complex. One possible signal transduction route is through the luminal Loop 7. The topology model of Scap reveals that Loop 1 and Loop 7 are the only two large loops on the lumenal side, with a great likelihood to interact with each other (Nohturfft et al., 1998b). The data present here strongly support this model.

We created a point mutation in Loop 1 (Y234A) or Loop 7 (Y640S) that rendered Scap unable to transport SREBPs to the Golgi complex even in the absence of sterols as revealed by SREBP processing assays and by immunofluorescence localization. In addition, the trypsin cleavage assay revealed that Loop 6 was in the closed conformation (i.e. the conformation that does not bind COPII proteins) in both mutants. But though Y234A protein is in the closed conformation, it still binds cholesterol with normal thermodynamics,

When expressed separately by co-transfection, Scap TM1-6 (including Loop 1) binds to Scap TM7-end (containing Loop 7) as determined by co-immunoprecipitation. When either the mutant TM1-6 segment or the mutant TM7-end segment was substituted for the corresponding WT segment, co-immunoprecipitation was abolished. This suggests that Loop 1 must interact with Loop 7. However, our initial efforts to detect direct interaction between purified recombinant Loop 1 and Loop 7 have so far been unsuccessful. Further studies are under way.

Cholesterol reproducibly reduced the co-immunoprecipitation between wildtype Scap TM1-6 and TM7-end by 50%; while 25-hydroxycholesterol had no effect even when Insig-1 was co-expressed. This might be explained by the observation that cholesterol directly binds Scap to block its movement; while 25-hydroxycholesterol blocks Scap movement not by binding to Scap, but rather by binding to Insig (Radhakrishnan et al., 2007).

There is a switch-like control of SREBP-2 transport triggered by small changes in the cholesterol level in ER membrane (Radhakrishnan et al., 2008). When ER cholesterol exceeds 5% of total ER lipids (molar basis), SREBP-2 transport is abruptly blocked. Transport resumes when ER cholesterol falls below the 5% threshold. It is important to understand how the luminal Loop1 and Loop7 in Scap sense a small ~2% difference in membrane cholesterol content and thereby elicit a profound conformational change. When cholesterol exceeds some threshold, it might become exposed from the membrane, allowing for recognition and response at the periphery of the membrane, where Scap Loop 1 lies.

In contrast to sterol mediated feedback inhibition of SREBP processing in mammals, phosphatidylethanolamine, the major phospholipid in *Drosophila*, controls the release of SREBP from *Drosophila* cell membranes, exerting feedback control on the synthesis of fatty acids and

phospholipids (Dobrosotskaya et al., 2002). This phospholipid sensing requires Scap with an unknown mechanism. In future, it would be worthwhile to determine that whether the luminal Loop1 and Loop7 in Scap is also involved in this process.

BIBLIOGRAPHY

- Adams, C.M., Reitz, J., De Brabander, J.K., Feramisco, J.D., Li, L., Brown, M.S., and Goldstein, J.L. (2004). Cholesterol and 25-hydroxycholesterol inhibit activation of SREBPs by different mechanisms, both involving SCAP and Insigs. *J Biol Chem* 279, 52772-52780.
- Brown, A.J., Sun, L., Feramisco, J.D., Brown, M.S., and Goldstein, J.L. (2002). Cholesterol addition to ER membranes alters conformation of SCAP, the SREBP escort protein that regulates cholesterol metabolism. *Mol Cell* 10, 237-245.
- Brown, M.S., Faust, J.R., Goldstein, J.L., Kaneko, I., and Endo, A. (1978). Induction of 3-hydroxy-3-methylglutaryl coenzyme A reductase activity in human fibroblasts incubated with compactin (ML-236B), a competitive inhibitor of the reductase. *J Biol Chem* 253, 1121-1128.
- Brown, M.S., and Goldstein, J.L. (1997). The SREBP pathway: regulation of cholesterol metabolism by proteolysis of a membrane-bound transcription factor. *Cell* 89, 331-340.
- Carstea, E.D., Morris, J.A., Coleman, K.G., Loftus, S.K., Zhang, D., Cummings, C., Gu, J., Rosenfeld, M.A., Pavan, W.J., Krizman, D.B., *et al.* (1997). Niemann-Pick C1 disease gene: homology to mediators of cholesterol homeostasis. *Science* 277, 228-231.
- Dobrosotskaya, I.Y., Seegmiller, A.C., Brown, M.S., Goldstein, J.L., and Rawson, R.B. (2002). Regulation of SREBP processing and membrane lipid production by phospholipids in *Drosophila*. *Science* 296, 879-883.
- Feramisco, J.D., Radhakrishnan, A., Ikeda, Y., Reitz, J., Brown, M.S., and Goldstein, J.L. (2005). Intramembrane aspartic acid in SCAP protein governs cholesterol-induced conformational change. *Proc Natl Acad Sci U S A* 102, 3242-3247.
- Gil, G., Faust, J.R., Chin, D.J., Goldstein, J.L., and Brown, M.S. (1985). Membrane-bound domain of HMG CoA reductase is required for sterol-enhanced degradation of the enzyme. *Cell* 41, 249-258.
- Gilbert, D.B., Tanford, C., and Reynolds, J.A. (1975). Cholesterol in aqueous solution: hydrophobicity and self-association. *Biochemistry* 14, 444-448.
- Goldstein, J.L., Basu, S.K., and Brown, M.S. (1983). Receptor-mediated endocytosis of low-density lipoprotein in cultured cells. *Methods Enzymol* 98, 241-260.
- Goldstein, J.L., DeBose-Boyd, R.A., and Brown, M.S. (2006). Protein sensors for membrane sterols. *Cell* 124, 35-46.
- Gong, Y., Lee, J.N., Lee, P.C., Goldstein, J.L., Brown, M.S., and Ye, J. (2006). Sterol-regulated ubiquitination and degradation of Insig-1 creates a convergent mechanism for feedback control of cholesterol synthesis and uptake. *Cell Metab* 3, 15-24.

Hannah, V.C., Ou, J., Luong, A., Goldstein, J.L., and Brown, M.S. (2001). Unsaturated fatty acids down-regulate srebp isoforms 1a and 1c by two mechanisms in HEK-293 cells. *J Biol Chem* 276, 4365-4372.

Horton, J.D., Goldstein, J.L., and Brown, M.S. (2002). SREBPs: activators of the complete program of cholesterol and fatty acid synthesis in the liver. *J Clin Invest* 109, 1125-1131.

Hua, X., Nohturfft, A., Goldstein, J.L., and Brown, M.S. (1996). Sterol resistance in CHO cells traced to point mutation in SREBP cleavage-activating protein. *Cell* 87, 415-426.

Ikeda, Y., Demartino, G.N., Brown, M.S., Lee, J.N., Goldstein, J.L., and Ye, J. (2009). Regulated endoplasmic reticulum-associated degradation of a polytopic protein: p97 recruits proteasomes to Insig-1 before extraction from membranes. *J Biol Chem* 284, 34889-34900.

Infante, R.E., Radhakrishnan, A., Abi-Mosleh, L., Kinch, L.N., Wang, M.L., Grishin, N.V., Goldstein, J.L., and Brown, M.S. (2008). Purified NPC1 protein: II. Localization of sterol binding to a 240-amino acid soluble luminal loop. *J Biol Chem* 283, 1064-1075.

Kapust, R.B., Tozser, J., Copeland, T.D., and Waugh, D.S. (2002). The P1' specificity of tobacco etch virus protease. *Biochem Biophys Res Commun* 294, 949-955.

Kita, T., Brown, M.S., and Goldstein, J.L. (1980). Feedback regulation of 3-hydroxy-3-methylglutaryl coenzyme A reductase in livers of mice treated with mevinolin, a competitive inhibitor of the reductase. *J Clin Invest* 66, 1094-1100.

Kwon, H.J., Abi-Mosleh, L., Wang, M.L., Deisenhofer, J., Goldstein, J.L., Brown, M.S., and Infante, R.E. (2009). Structure of N-terminal domain of NPC1 reveals distinct subdomains for binding and transfer of cholesterol. *Cell* 137, 1213-1224.

Motamed, M., Zhang, Y., Wang, M.L., Seemann, J., Kwon, H.J., Goldstein, J.L., and Brown, M.S. (2011). Identification of luminal Loop 1 of Scap protein as the sterol sensor that maintains cholesterol homeostasis. *J Biol Chem* 286, 18002-18012.

Nohturfft, A., Brown, M.S., and Goldstein, J.L. (1998a). Sterols regulate processing of carbohydrate chains of wild-type SREBP cleavage-activating protein (SCAP), but not sterol-resistant mutants Y298C or D443N. *Proc Natl Acad Sci U S A* 95, 12848-12853.

Nohturfft, A., Brown, M.S., and Goldstein, J.L. (1998b). Topology of SREBP cleavage-activating protein, a polytopic membrane protein with a sterol-sensing domain. *J Biol Chem* 273, 17243-17250.

Nohturfft, A., Yabe, D., Goldstein, J.L., Brown, M.S., and Espenshade, P.J. (2000). Regulated step in cholesterol feedback localized to budding of SCAP from ER membranes. *Cell* 102, 315-323.

Porter, J.A., Young, K.E., and Beachy, P.A. (1996). Cholesterol modification of hedgehog signaling proteins in animal development. *Science* 274, 255-259.

Radhakrishnan, A., Goldstein, J.L., McDonald, J.G., and Brown, M.S. (2008). Switch-like control of SREBP-2 transport triggered by small changes in ER cholesterol: a delicate balance. *Cell Metab* 8, 512-521.

Radhakrishnan, A., Ikeda, Y., Kwon, H.J., Brown, M.S., and Goldstein, J.L. (2007). Sterol-regulated transport of SREBPs from endoplasmic reticulum to Golgi: oxysterols block transport by binding to Insig. *Proc Natl Acad Sci U S A* 104, 6511-6518.

Radhakrishnan, A., Sun, L.P., Kwon, H.J., Brown, M.S., and Goldstein, J.L. (2004). Direct binding of cholesterol to the purified membrane region of SCAP: mechanism for a sterol-sensing domain. *Mol Cell* 15, 259-268.

Rawson, R.B., DeBose-Boyd, R., Goldstein, J.L., and Brown, M.S. (1999). Failure to cleave sterol regulatory element-binding proteins (SREBPs) causes cholesterol auxotrophy in Chinese hamster ovary cells with genetic absence of SREBP cleavage-activating protein. *J Biol Chem* 274, 28549-28556.

Sakai, J., Nohturfft, A., Cheng, D., Ho, Y.K., Brown, M.S., and Goldstein, J.L. (1997). Identification of complexes between the COOH-terminal domains of sterol regulatory element-binding proteins (SREBPs) and SREBP cleavage-activating protein. *J Biol Chem* 272, 20213-20221.

Sever, N., Song, B.L., Yabe, D., Goldstein, J.L., Brown, M.S., and DeBose-Boyd, R.A. (2003a). Insig-dependent ubiquitination and degradation of mammalian 3-hydroxy-3-methylglutaryl-CoA reductase stimulated by sterols and geranylgeraniol. *J Biol Chem* 278, 52479-52490.

Sever, N., Yang, T., Brown, M.S., Goldstein, J.L., and DeBose-Boyd, R.A. (2003b). Accelerated degradation of HMG CoA reductase mediated by binding of insig-1 to its sterol-sensing domain. *Mol Cell* 11, 25-33.

Skalnik, D.G., Narita, H., Kent, C., and Simoni, R.D. (1988). The membrane domain of 3-hydroxy-3-methylglutaryl-coenzyme A reductase confers endoplasmic reticulum localization and sterol-regulated degradation onto beta-galactosidase. *J Biol Chem* 263, 6836-6841.

Sun, L.P., Li, L., Goldstein, J.L., and Brown, M.S. (2005). Insig required for sterol-mediated inhibition of Scap/SREBP binding to COPII proteins in vitro. *J Biol Chem* 280, 26483-26490.

Sun, L.P., Seemann, J., Goldstein, J.L., and Brown, M.S. (2007). Sterol-regulated transport of SREBPs from endoplasmic reticulum to Golgi: Insig renders sorting signal in Scap inaccessible to COPII proteins. *Proc Natl Acad Sci U S A* 104, 6519-6526.

Tessier, D.C., Thomas, D.Y., Khouri, H.E., Laliberte, F., and Vernet, T. (1991). Enhanced secretion from insect cells of a foreign protein fused to the honeybee melittin signal peptide. *Gene* 98, 177-183.

Wang, M.L., Motamed, M., Infante, R.E., Abi-Mosleh, L., Kwon, H.J., Brown, M.S., and Goldstein, J.L. (2010). Identification of surface residues on Niemann-Pick C2 essential for hydrophobic handoff of cholesterol to NPC1 in lysosomes. *Cell Metab* 12, 166-173.

Wei, J.H., and Seemann, J. (2009a). Induction of asymmetrical cell division to analyze spindle-dependent organelle partitioning using correlative microscopy techniques. *Nature protocols* 4, 1653-1662.

Wei, J.H., and Seemann, J. (2009b). The mitotic spindle mediates inheritance of the Golgi ribbon structure. *J Cell Biol* 184, 391-397.

Yabe, D., Brown, M.S., and Goldstein, J.L. (2002a). Insig-2, a second endoplasmic reticulum protein that binds SCAP and blocks export of sterol regulatory element-binding proteins. *Proc Natl Acad Sci U S A* 99, 12753-12758.

Yabe, D., Xia, Z.P., Adams, C.M., and Rawson, R.B. (2002b). Three mutations in sterol-sensing domain of SCAP block interaction with insig and render SREBP cleavage insensitive to sterols. *Proc Natl Acad Sci U S A* 99, 16672-16677.

Yamamoto, T., Davis, C.G., Brown, M.S., Schneider, W.J., Casey, M.L., Goldstein, J.L., and Russell, D.W. (1984). The human LDL receptor: a cysteine-rich protein with multiple Alu sequences in its mRNA. *Cell* 39, 27-38.

Yang, T., Espenshade, P.J., Wright, M.E., Yabe, D., Gong, Y., Aebersold, R., Goldstein, J.L., and Brown, M.S. (2002). Crucial step in cholesterol homeostasis: sterols promote binding of SCAP to INSIG-1, a membrane protein that facilitates retention of SREBPs in ER. *Cell* 110, 489-500.

Yang, T., Goldstein, J.L., and Brown, M.S. (2000). Overexpression of membrane domain of SCAP prevents sterols from inhibiting SCAP.SREBP exit from endoplasmic reticulum. *J Biol Chem* 275, 29881-29886.

Zhang, Y., Motamed, M., Seemann, J., Brown, M.S., and Goldstein, J.L. (2013). Point mutation in luminal loop 7 of Scap protein blocks interaction with loop 1 and abolishes movement to Golgi. *J Biol Chem* 288, 14059-14067.